Understanding the Mechanism of Injury Associated with Long Bone Fractures Through Dynamic Bending Impact

by

Toshika Sheshna Emrith

EMRTOS001

SUBMITTED TO THE UNIVERSITY OF CAPE TOWN

In partial fulfilment of the requirements for the degree

Master of Philosophy (MPhil) Biomedical Forensic Science

University of Cape Town

Supervised by:

Mr Calvin Mole

Dr Marise Heyns

Division of Forensic Medicine and Toxicology

Department of Pathology

Faculty of Health Sciences

The copyright of this thesis vests in the author. No quotation from it or information derived from it is to be published without full acknowledgement of the source. The thesis is to be used for private study or non-commercial research purposes only.

Published by the University of Cape Town (UCT) in terms of the non-exclusive license granted to UCT by the author.

University of Cape Town

DECLARATION

I, **Toshika Sheshna Emrith,** hereby declare that this submission is my own work and that, to the best of my knowledge and belief, it contains no material previously published or written by another person and that neither the whole work nor any part of it has been, is being, or is to be submitted for another degree or diploma in this or any other university, except where due acknowledgement has been made in the text.

I empower the university to reproduce for the purpose of research either the whole or any portion of the contents in any matter whatsoever.

Signed by candidate

Toshika Sheshna Emrith

22/04/2019

PLAGIARISM DECLARATION

I know that plagiarism is wrong. Plagiarism is to use another's work and pretend that it is one's own.

I have used the Harvard convention for citation and referencing. Each contribution to, and quotation in, this dissertation the work(s) of other people has been attributed and has been cited and referenced.

This dissertation is my own work.

I have not allowed, and will not allow, anyone to copy my work with the intention of passing it off as his or her own work.

SIGNATURE Signed by candidate

DATE 22/04/2019

ABSTRACT

Blunt force trauma may result from homicide and assault cases, child abuse and motor vehicle accidents. Such incidents often result in skeletal trauma. Trauma to the lower limbs due to bending forces often involves a fracture pattern known as a butterfly or wedge fracture. Forensic analysis of the butterfly fracture aids in the establishment of directionality of the force applied. Currently, forensic anthropologists employ a method dictating that the base of the butterfly fragment pertains to the side of impact, while the apex of the fragment pertains to the opposite side of impact. Recent studies have demonstrated that this theory leads to erroneous forensic reconstructions as it assumes that all butterfly fractures are produced due to bone failing in tension. Furthermore, it requires the presence of a detached piece in order to be applicable, which is also the case for other proposed methods.

The current study explores the biomechanics involved in the production of butterfly fractures by conducting 3-point bending impacts through a drop apparatus. It also investigates the accuracy of current and proposed forensic methods and aims at establishing a more reliable method of inferring directionality from the fracture pattern. From the sample fractured in this study, 11.8% of the fractures produced were tension wedges and 14.7% were compression wedges. When applying the existing methods of inferring directionality to the fractured sample, the accuracies ranged from 5.9% to 59%, while the method developed during this study achieved an accuracy of 97.1%.

These results highlight the need of considering compression wedges during forensic reconstructions and understanding the impact of employing methods conceptualised on the assumption that all butterfly wedges are produced in tension.

ACKNOWLEDGEMENTS

Mr Calvin Mole:

I am privileged to have had a mentor like you. There are no words to describe my gratitude towards your kindness, unwavering support and endless patience. I have had the opportunity to learn so much while under your care. This work could have never been completed without your untiring help. I am so thankful for your understanding and for not giving up on me during the hard times. And thank you for lending me the Dremel and allowing me to develop my drilling and sawing skills, and for introducing me to the gross art of bone maceration!

Dr Marise Heyns:

You have been my rock throughout this entire degree. Your selflessness is one of a kind. Thank you for having always been so inspiring and encouraging. I will never forget the numerous times I came to your office filled with worry and how you never failed to offer me a shoulder to lean on. Your support was indispensable during my time in the division.

My Old Man:

It is said that daughters are the closest to their dads. I cannot think of a better example than the two of us. Thank you for having always encouraged me to follow my own path and for teaching me never to be scared of taking risks or when presented with mountainous obstacles. I would never have been able to face the challenges if it was not for your unwavering faith in me. You have always believed in me even when I could no longer believe in myself and I am forever grateful to you for that. Love you Papi.

My Emotional Lady:

I am incredibly lucky to have a woman like you looking over me. Your ever-growing love and caring nature have never failed to be by my side, especially when I needed them the most. Thank you for your determination in making sure that I know I am not alone even when I am far from home. Love you Mami.

To the Division of Forensic Medicine and Toxicology Team:

You guys are awesome! Thank you for all the good times and the support during the hard times.

Table of Contents

List of Figures

List of Tables

1. INTRODUCTION

1.1 Importance of Forensic Anthropology

Anthropology, derived from the Greek words *Anthropos* and *Logia,* meaning “human” and “study of” respectively, strives to understand mankind in all its aspects. One subdiscipline of anthropology is biological anthropology, which focusses on the biological origins of humans along with the adaptation and variation of mankind throughout evolution. Forensic anthropology is thereby an extension of biological anthropology (Tersigni-Tarrant and Shirley, 2013). It is defined as a multidisciplinary field combining expertise in physical anthropology, physics and anatomy, to provide evidence pertaining to the identity of the victim and the mechanisms of injury which may have occurred as a result of a violent death (Kimmerle and Baraybar, 2008; Iscan and Steyn, 2013).

Forensic anthropologists are tasked with reconstructing the biological identity of the victim, as well as identifying skeletal trauma which may have occurred antemortem, perimortem and postmortem. The reconstruction of the biological identity, also referred to as the biological profile of an individual, involves the application and understanding of phases of skeletal growth, maturity and degeneration to ascertain sex, ancestry and stature of the victim. Analysis of skeletal variation further strengthens the possibility of an accurate victim identification (Tersigni-Tarrant and Shirley, 2013).

Forensic anthropologists also engage in the analysis of trauma associated with the skeletal remains. The analysis and interpretation of trauma aids in the reconstruction of forensic cases pertaining to violent deaths, by providing insights into the circumstances surrounding death (Kimmerle and Baraybar, 2008; Tersigni-Tarrant and Shirley, 2013). Three main questions are usually answered through the interpretation of trauma:

1) Identification of skeletal abnormalities to infer time of injury (ante-/ peri-/ post-mortem)
2) Identification of the biomechanics involved in the production of fractures
3) Interpretation of sequence of events that may have led to death

Furthermore, differentiation between antemortem and peri/postmortem trauma may strengthen the robustness of establishing a positive victim identification (Iscan and Steyn, 2013). Identification of antemortem trauma may act as unique identifiers as they pertain to the lifestyle of an individual. This helps in narrowing the pool of possible identities generated by the establishment of sex, age and ancestry. Forensic anthropologists therefore, require an enhanced knowledge of the human skeletal anatomy to differentiate between normal morphological variations and defects pertaining to trauma of the hard tissue (Kimmerle and Baraybar, 2008; Tersigni-Tarrant and Shirley, 2013). Trauma analysis also requires the application of biomechanical principles to accurately reconstruct the mechanism of injury involved in the production of skeletal trauma (Symes *et al.*, 2012; Wedel and Galloway, 2013). Analysis of trauma patterns and mechanism of injury not only aids in criminal proceedings but also assists in uncovering violations pertaining to human right laws such as genocides and war crimes (Kimmerle and Baraybar, 2008).

Consequently, in the absence of soft tissue, medicolegal practitioners require the assistance of forensic anthropologists to accurately document, analyse, explain and reconstruct the patterns of trauma in cases of violent deaths such as homicides, mass fatalities and genocides (Davidson *et al.*, 2011). To this end, much focus has been placed on the analysis of trauma to refine our understanding of the human skeletal system and hence, to better assist law enforcement and human rights agencies (Iscan and Steyn, 2013; Kimmerle and Baraybar, 2008). Forensic anthropology is therefore, of evidential value in both criminal and non-criminal investigations, as well as natural catastrophes, war crimes and genocide investigations (Davidson *et al.*, 2011).

1.1.1 Trauma to Long Bones

One of the leading causes of mortality involving skeletal trauma is blunt force (Symes *et al.*, 2012; Wedel and Galloway, 2013). Forensic samples involving blunt force trauma to the lower extremities may include victims of homicidal assault, child abuse, motor vehicle accidents and falls, amongst others (Galloway and Zephro, 2005). While accurately establishing cause of death from skeletal samples alone is a difficult and strenuous task, forensic anthropologists may distinguish between the possible causes and conclusively ascertain the circumstances leading to death based on the pattern of trauma pertained to the skeleton (Christensen and Smith, 2013; Lefèvre *et al.,* 2015).

An understanding of fracture patterns is, therefore, highly valuable for anthropological reconstructions. Long bones exposed to blunt force trauma often result in fracture patterns such as crush, transverse, oblique, spiral and butterfly (Gozna *et al.*, 1982). Forensic anthropologists study the different mechanisms involved in the production of the above-mentioned fractures to understand more about the velocity, force and directionality of the blow (Kimmerle and Baraybar, 2008; Symes *et al.*, 2012; Sharkey *et al.*, 2011; Kieser *et al.*, 2013).

Victims of homicidal assaults usually exhibit low numbers of highly localised crush fractures as a result of being impacted by an instrument, in combination to damage to the head and torso. Child abuse is usually identified by a high number of repetitive diaphyseal and epiphyseal fractures, both recent and healed, to the lower limbs (Galloway and Zephro, 2005). Motor vehicle accidents and falls are known to exhibit a fairly similar pattern of blunt force injuries and can be difficult to distinguish from one another (Wedel and Galloway, 2013; Lefèvre *et al.*, 2015). Of importance is the butterfly/wedge fracture as the latter is highly prominent in motor vehicle accidents, more specifically in pedestrians (Teresinski and Madro, 1999; Schmidt *et al.*, 2016). Wedge fractures are produced as a result of the pedestrian being impacted on the lower limbs by the car bumper, causing bending (Rastogi *et al.*, 1986). These fractures are therefore highly valuable pieces of evidence in forensic reconstructions involving blunt force trauma as not only do they aid in the distinction between motor vehicle accidents and falls, but they also assist with determining the position of the victim and force/speed of the impact (Teresinski and Madro, 1999; Schmidt *et al.*, 2016).

While the mechanism of injury of transverse, oblique and spiral fractures are well established, a high degree of uncertainty still prevails around the formation of wedge fractures (Reber and Simmons, 2015; Isa *et al.*, 2017). The current method of reconstructing wedge fractures and inferring directionality being used by forensic anthropologists dates to the 1880s, where it has been widely accepted that the base of the wedge piece pertains to the site of impact (compression), and the apex of the piece pertains to the site of initial failure (tension) (Messerer, 1880). Based on these parameters, the direction of impact could be ascertained, with the apex of the wedge fracture pointing in the direction the force was applied.

This theory has since been proven to be only 60% accurate, thereby leading to erroneous reconstructions (Reber and Simmons, 2015; Schmidt *et al.*, 2016; Isa *et al.*, 2017). Research, along with the analysis of real-life case studies, have shown that in certain cases, initial failure may arise at the site of impact (compression) (Rabl *et al.*, 1996; Teresinski and Madro, 1999). This shows that although theoretically, the method put forward by Messerer extensively explains the production of wedge fractures, it should be regarded as a hypothesis and therefore, requires further research.

1.2 Skeletal Trauma

Skeletal trauma, commonly materialised as dislocations and/or fractures, can be defined as an injury or modification to the hard tissue caused by the application of extrinsic parameters such as energy and force (Lovell, 1997; Symes *et al.,* 2012). The axiom behind the basis of skeletal trauma analysis is that the damage sustained is dependent on the level of energy impacting the bone. Forensic anthropologists, therefore, classify skeletal trauma into three main categories based on the level and shape of the damage perceived in bone, along with the directionality of force and energy. Those categories are ballistics/gunshot trauma, sharp force trauma and blunt force trauma (Symes *et al.*, 2012; Davidson *et al.*, 2011; Wedel and Galloway, 2013).

Ballistic trauma is attributed to damages sustained under rapid loading conditions, usually from a fired bullet, resulting in shattering of the affected area and/or bevelling. Sharp force trauma is defined as a slow loading compressive force from a sharp object, acting on a narrowly focused area, producing injuries that resulted from bone being penetrated by a sharp edge or point (Symes *et al.*, 2012; Davidson *et al.*, 2011). The damage usually takes the form of incisions. Blunt force trauma is similar to sharp force trauma in that they both result from slow loading forces. Blunt force trauma can manifest as direct or indirect trauma. Direct trauma is defined as a break happening at the point of impact, resulting in transverse, comminuted or crush fractures. Indirect trauma is a result of combining tension, compression and shear forces resulting in a fracture at a point different from the point of impact. Indirect trauma to long bones includes spiral and butterfly fractures (Lovell, 1997; Galloway and Zephro, 2005; Symes *et al.*, 2012).

For a better understanding on the mechanisms involved in blunt force trauma, knowledge about bone characteristics and its biomechanics is firstly required.

1.3 Bone as a Composite Material

Bone is defined as a calcified connective tissue whereby its material structures work in synergy to provide mechanical support, assist with biological functions such as blood production, storage for calcium and phosphorus and chemical functions such as mineral ion homeostasis (Rho *et al.*, 1998). It is a heterogenous composite comprising of 60% inorganic material, 30% organic material and 10% extracellular matrix (Mubeen *et al.*, 2015). There is an understanding that these material structures along with bone's internal architecture have throughout the evolutionary years worked together to allow bone to better adapt to its load-bearing function (Ruff *et al.*, 2006). This principle is referred to in the literature as "Wolff's Law", more commonly known as the law of remodelling. It stipulates that both the internal and external architecture of bone will undergo alterations as a result of the application of stress (Wolff, 1982). An example of this law is given in Lanyon *et al.*, (1982) where bone undergoing increased strain will experience an increase in bone deposition while bone experiencing decreased strain will undergo bone resorption.

1.3.1 Bone Hierarchical Structure

In adult bones, the organic phase makes up nearly 30% of the matrix by volume. It comprises mostly of fibrillar type I collagen, along with a small percentage of glycoproteins and non-collagenous proteins. The mineral phase, making up around 60% of bone tissue by volume, consists primarily of hydroxyapatite crystals, $Ca_{10}(PO_4)_6(OH)_2$, formed by the chemical interactions between calcium phosphate and calcium hydroxide. Bone tissue also contains water, amorphous polysaccharides, blood vessels and cells which form part of the extracellular matrix (Katz and Li, 1973; Oyen and Ferguson, 2010; Kieser *et al.*, 2013;). The interplay between the three main constituents of bone has a primary effect on the mechanical properties of bone (Currey, 2003b). Rho *et al.* (1998) and Reznikov *et al.* (2014) summarise the different

levels of bone hierarchical structure. These are described below in descending order as summarised in Figure 1.1.

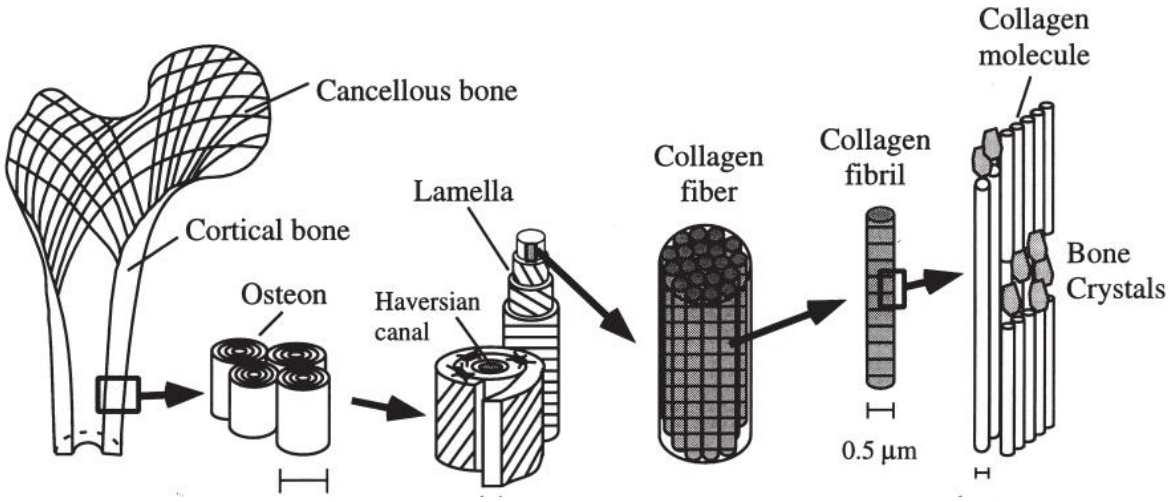

Figure 1.1

Diagrammatical summary of the hierarchical structure of bone (Rho et al., 1998)

(i) <u>Macrostructure</u>

The macrostructures congregate differently to form four different shapes of bone, namely, long bones, short bones, flat bones and irregular bones. Long bones are longer than they are wide and are usually found in the upper and lower limbs. They consist of a shaft, referred to as the diaphysis and two articular ends, known as the epiphyses. The centre of the diaphysis is usually hollow, consisting of a medullary cavity. During the fifth intra-uterine week, ossification begins, resulting in poorly organised bone tissue commonly referred to as woven bone, which has a high organic content compared to mineral content (Oyen and Ferguson, 2010; Hipp and Hayes, 2013; Wedel and Galloway, 2013). These later mature into either trabecular (spongy) bone, which is the low-density form of bony tissue (0.05-1.0 g/cc) or as cortical (compact) bone, which is its high density form (18-2.0 g/cc) (Porta, 2005). Taking the femur as an example, trabecular bone is more prominent internally at the articular ends while cortical bone makes up the external shaft of the skeletal element. The percentage composition of trabecular to cortical bone varies from bone to bone, thereby accounting for their different functions. When looking at the cross section of a

femur, the outer layer is made up of compact bone, while the inner layer comprises of trabecular bone (Figure 1.2). The two bone types are primarily differentiated by their degree of porosity. Trabecular bone exhibits bony struts and cavities, while cortical bone takes the form of a smooth, compressed plate. Trabecular bone has a higher surface area to volume ratio than cortical bone because it is less dense. Metabolically and mechanically, trabecular bone is more active, undergoes faster remodelling and is a better stress absorber than cortical bone.

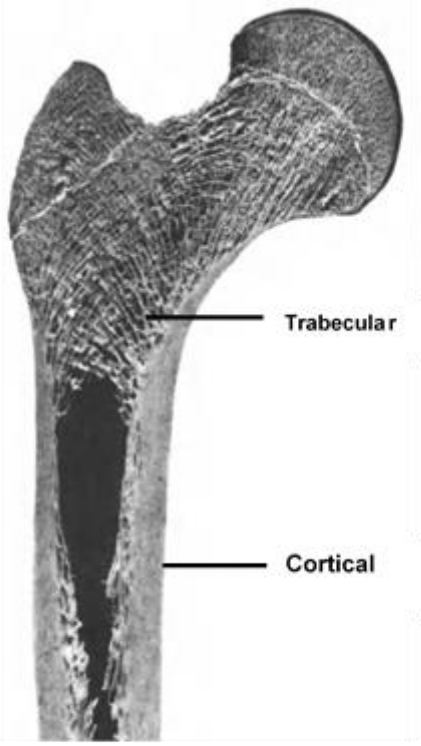

Figure 1.2

Photograph of the cross section of a femur along the coronal plane. Picture adapted from (Wolff, 1982)

(ii) *Microstructure*

When examined under a microscope, bone can further be broken down into lamellar bone, woven bone (Figure 1.3) and trabeculae (Figure 1.4). These are differentiated by the arrangement and orientation of bundles of mineralised collagen fibrils (Katz and Li, 1973). In lamellar bone, the fibril bundles are present in an orderly manner, following a unidirectional planar arrangement, forming what is commonly described as a plywood-type stacking of thick layers. A second, less common, arrangement of

lamellar bone involves a gradual change in the orientation of the bundle layers, usually described as twisted plywood. The organised, stacked layers in both arrangements are separated by woven bone. While lamellar bone is made of organised fibril bundles, woven bone on the other hand, is made of fibril bundles arranged in a disorderly manner. It acts as a precursor to lamellar bone during bone development, as well as during fracture repair. One common example of woven bone is callus formation during bone healing. Trabeculae are the defining structures of trabecular bone. These are rod and/or plate like structures that are arranged in a way that allows trabecular bone to absorb stress.

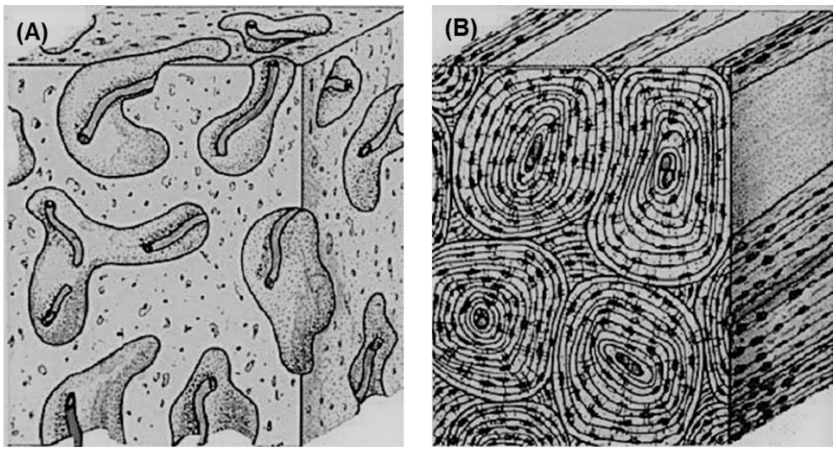

Figure 1.3

(A)Woven Bone ***(B)*** *Lamellar Bone*

Diagrams adapted from (Safadi et al. 2009)

Another important microstructure of bone is the Haversian system, also known as secondary osteons. These are cylindrical structures running perpendicularly to the arrangement of lamellar bone, measuring 100-200 μm in diameter, with a central canal of approximately 30-40 μm in diameter (Sharir *et al.*, 2008). The Haversian systems are identified by concentric formations of lamellar bone around the central canal, as depicted in Figure 1.4.

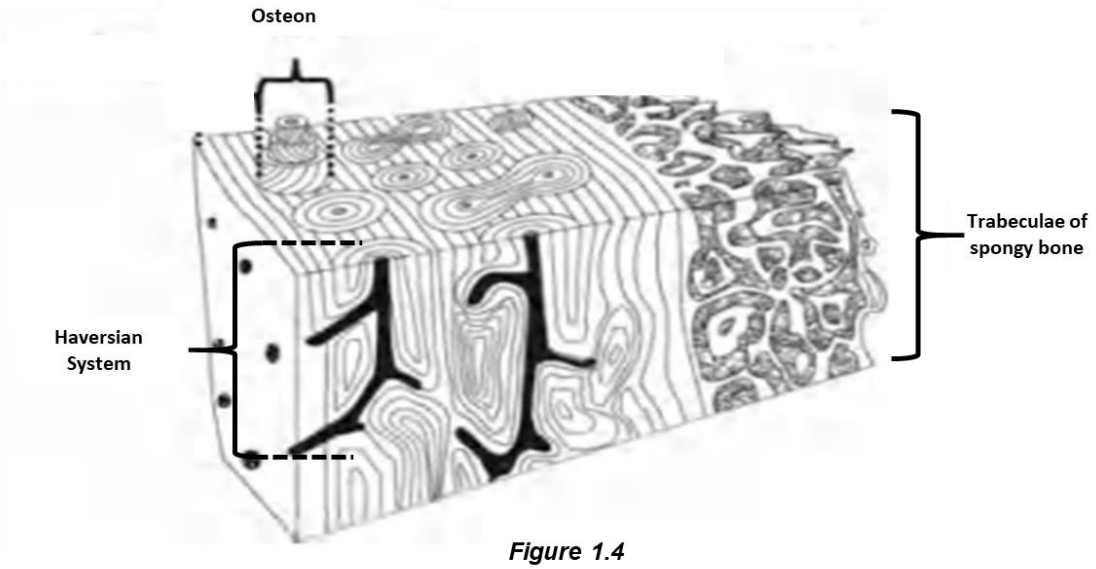

Figure 1.4

Schematic representation of bone microstructure depicting Haversian systems and trabeculae of trabecular bone. Diagram adapted from (Kieser et al., 2013)

(iii) Sub-Microstructure

Osteoblasts are bone cells involved in the formation of bone tissue. The production of osteoblasts is triggered when bone undergoes stress, either mechanical or metabolic (Martin *et al.*, 1998). The main function of osteoblasts is to produce osteoids, which comprise of collagen, proteins and water. These combine to form the non-mineralised organic section of the bone matrix. After being encased in the bone matrix, osteoblasts transform into osteocytes, commonly referred to as the mature bone cells (Martin *et al.*, 1998; Porta, 2005). Lamellae are dense, interwoven collagen fibril bundles which make up the different bone types, described in Section 1.3.1(ii). Osteocytes, usually found between the spaces of neighbouring lamellae, are responsible for the maintenance of bone tissue and are arranged in between bone pores known as lacunae. A network of little canals (*canaliculi*) connects the osteocytes together and allows them to interact with each other (Figure 1.5). Lastly, bone resorption is performed by osteoclasts. These occur in spaces known as Howship's lacunae (Figure 1.6) (Tersigni-Tarrant and Shirley, 2013).

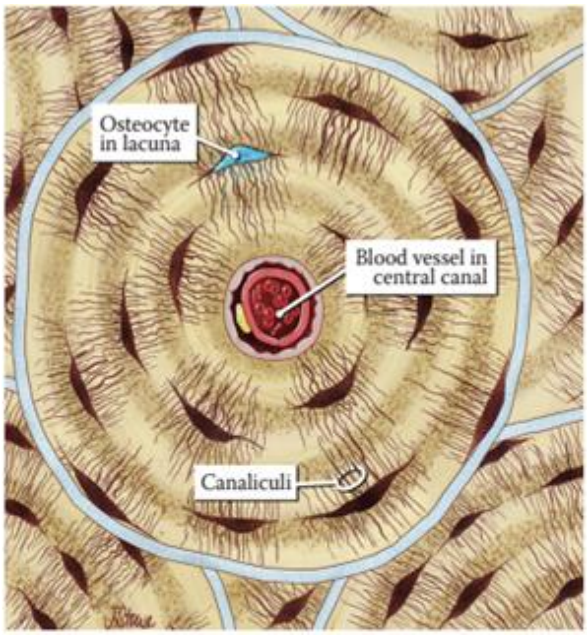

Figure 1.5

Schematic representation of a network of canaliculi and lacunae forming an osteon. Diagram adapted from (Tersigni-Tarrant and Shirley, 2013)

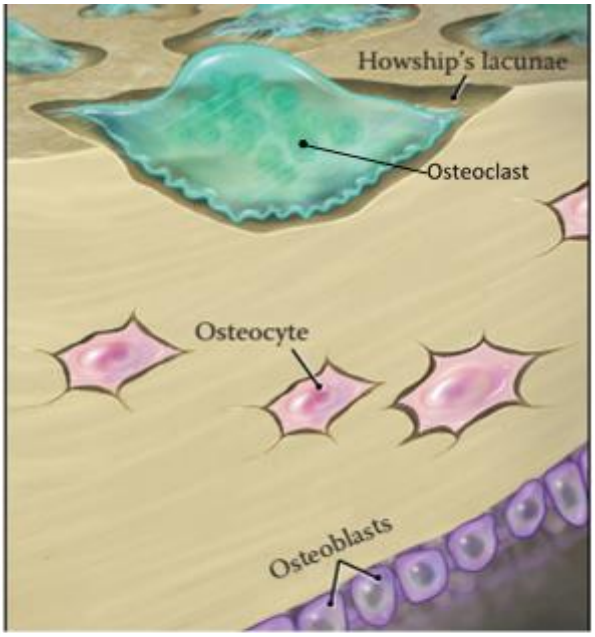

Figure 1.6

Schematic representation of bone cells. Diagram adapted from (Tersigni-Tarrant and Shirley, 2013)

(iv) *Nano Structure*

At this level, the building blocks of bone are discernible, namely collagen molecules and calcium hydroxyapatite crystals. Type I collagen molecules covalently bond with calcium hydroxyapatite crystals to form mineralised collagen fibrils which vary between 80 and 100 nm in diameter, while the crystals measure around 50 nm in length, 25 nm in width and 3 nm in thickness (Sharir *et al.*, 2008).

The arrangement of the material structures in long bones thereby dictate the mechanical properties of these bones, such as strength and resistance, and their response to impact.

1.4 Bone Biomechanics

The analysis of skeletal trauma makes use of the principles of physics and mechanics as applied to the human body, hence known as biomechanics. To fully interpret trauma on bone it is necessary to first have an understanding of how that trauma came to be and the underlying mechanism thereof. Therefore, a basic understanding of the principles and terminologies of mechanics is required. These principles are well defined by Young *et al.,* (2008), a summary of which can be found below.

1.4.1 Terminology and Principles

(i) Force

In layman's terms, a force is described as a push or a pull, but as defined by Newton's second law of motion, when bone is impacted with an implement (m), the force (F) generated will result in an acceleration (a), defined as the rate of change in velocity, in the motion of said mass. The acceleration is considered to be directly proportional in magnitude to the applied force. In other words, when force is applied to bone, it will result in a change in motion of its internal elements, thereby resulting in a change in shape and/or size (Porta, 2005).

$$\vec{F} = ma$$ **; [SI unit: N; Derived unit: kg.ms^{-2}]**

(ii) Stress

Stress (σ) is a quantity which characterises the strengths of forces acting upon bone, eventually resulting in deformation. It is usually measured in a force per unit area basis.

Stress = Force/Area [SI unit: Pa; Derived unit: N/m^2]

σ = F/A

Stress can be classified into three main categories based on the nature of the force: tension, compression and shear (Figure 1.7).

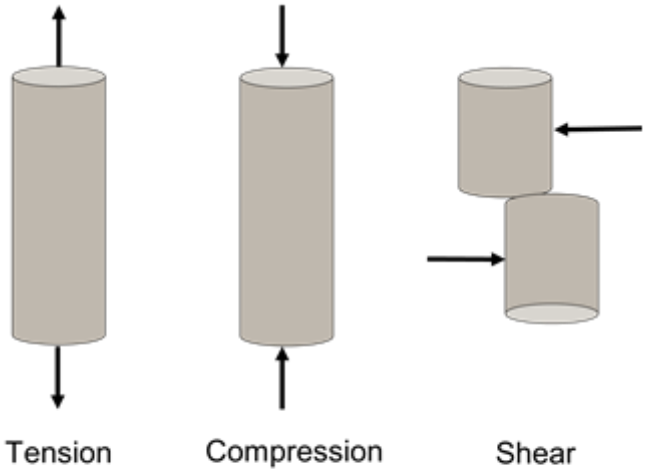

Figure 1.7

Types of stresses that may act upon an object.

It is said that an object is subjected to **tensile stress/ tension** when two forces equal in magnitude, but acting in opposite directions, move away from the centre of the structure. This causes the object to lengthen, thereby becoming narrower along the axis undergoing tension. In bone, tensile forces result in the separation of the osseous tissue and triggers the propagation of fracture lines. One of the most common examples of bone undergoing pure tensile forces is the production of avulsion fractures. In the lower extremity, pure tensile fractures are usually found around the trochanters of the femur, the tibial tuberosity and the patella (Porta, 2005). Avulsion fractures can be found in cases of child abuse, when one extremity of the child was pulled, resulting in fracture (Symes *et al.*, 2012).

Compressive stress/ compression is when two opposite forces of equal magnitude act towards the centre of a bone, causing the skeletal element to widen and shorten, resulting in constriction of the bone. Even though bone is highly resistant to compressive forces, an excess of compression may result in the production of a buckling fracture, as the resilience is exceeded (Galloway and Zephro, 2005). Buckling fractures may occur as a result of a fall from a great height (Davidson *et al.*, 2011).

Shear stress occurs when two opposite forces of equal magnitude act parallel to each other, resulting in angular deformation of the structure.

In reality, fractures do not usually occur strictly due to pure tension, compression or shear. Rather, they occur as a result of a combination of the above-mentioned stress forces.

Torsion is a combination of shear and tension. When bone is twisted, the epiphyses act as anchor points causing the diaphysis to rotate. This initiates the production of a longitudinal fracture line which curves at a 45° angle around the shaft of the bone. The most common fracture due to torsion in long bones is the spiral fracture (Martin *et al.*, 1998; Galloway and Zephro, 2005).

Bending is a common fracture mechanism in lower limb bones. When the diaphysis is impacted transversely, bone behaves like a classic beam. The epiphyses act as anchor points, causing the diaphysis to bend. Consequently, bone experiences a combination of compressive and tensile forces. The impact point undergoes compression, while the opposite side undergoes tension. A neutral plane of zero stress occurs between the two forces. As stress is applied further, bone undergoes failure. Common fractures during bending are wedge fractures, oblique and transverse fractures (Alms, 1961; Porta, 2005).

(iii) *Strain*

When bone experiences stress, it undergoes deformation. Strain (ε) is a measure of deformation and is interpreted as a ratio in the change in length of an object. As a ratio it has no units.

Strain = Change in length/Original length

$$\varepsilon = \delta L/L$$

(iv) *Relationship of stress and strain*

The relationship between stress and strain can be used as an indication of bone's stiffness (Currey 2003a), defined by a constant known as *Young's Modulus* (E). A diagrammatic representation of this relationship is known as the stress-strain curve (Figure 1.8).

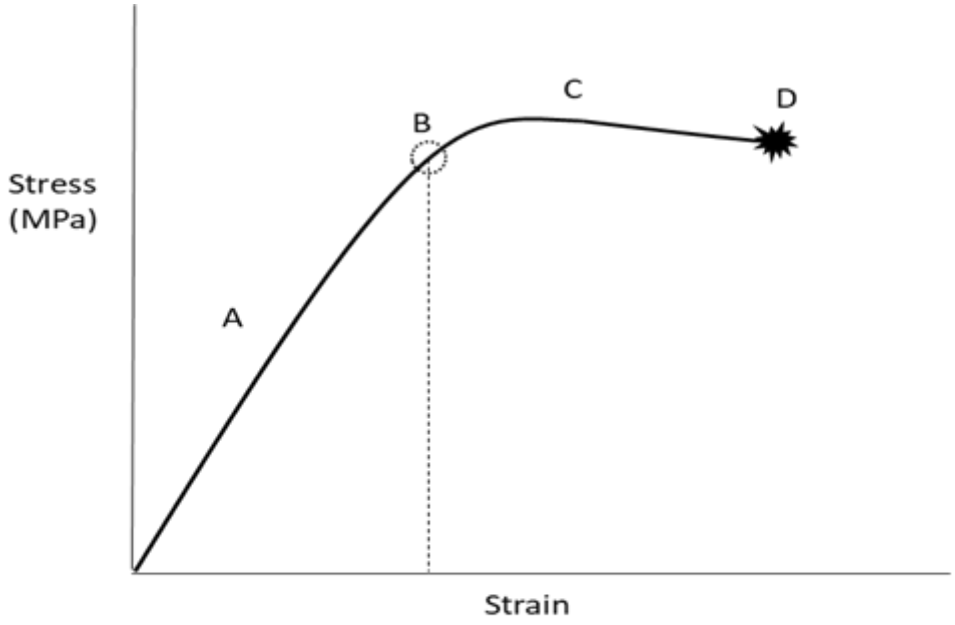

Figure 1.8

*Graphical representation of the relationship between stress and strain of an anisotropic object. **(A)** is the elastic phase, where strain is directly proportional to stress; **(B)** is the yield point; **(C)** shows the plastic phase leading to failure **(D)**. Area under the graph*

Stress and strain experienced prior to the yield point determines how much energy bone is able to withstand without undergoing any irreversible deformation. The yield point is also defined as bone's limit of elasticity. Prior to reaching the yield point, bone behaves in an elastic manner, where the resulting strain is linearly proportional to the experienced stress. As the elastic limit is exceeded, bone enters the plastic phase or the post yield phase. This defines the amount of energy that can be absorbed by bone before failure. During the post yield phase, deformation experienced is irreversible and results in the initiation of microfractures. As stress increases to the maximum, bone reaches closer to its ultimate tensile strength, which, when exceeded, results in a complete fracture (Currey, 2003b; Porta, 2005).

For composite materials such as bone, the relationship between stress and strain is more complex. Bone is known as an **anisotropic** material. This is due to the combination of organic and inorganic materials (Section 1.3), along with its non-uniform shape. In simple terms, it is said that bone behaves differently depending on the angle of impact. This relates to bone being more resistant to compressive forces than tensile forces (Porta, 2005). Furthermore, the elastic properties of anisotropic

materials differ depending on the loading direction. As a consequence, bone has more than one elastic modulus, each one related to the loading direction, implying that the elastic modulus of a long bone when loaded parallel to its longitudinal axis is greater than the elastic modulus of the same bone when loaded perpendicularly to its longitudinal axis (Martin *et al.*, 1998). Figure 1.9 demonstrates the stress and strain curves for different materials, both brittle and elastic, in relation to bone.

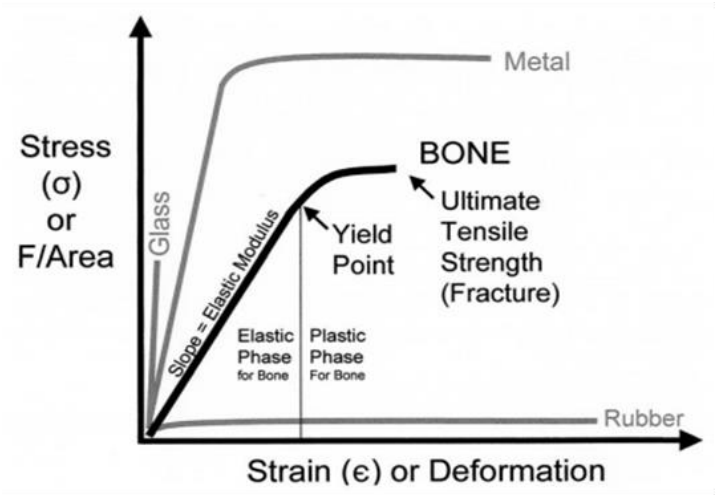

Figure 1.9
Stress-Strain curve for different materials. Rubber is isotropic and therefore behaves in a linearly elastic manner. Bone is anisotropic and therefore has both an elastic and plastic phase (Porta, 2005).

(v) *Work*

Work (W) done can be defined as the product of force (F) on an object and the distance covered by the object as a result. For bone, work or energy needed to initiate a fracture can also be defined as its toughness (Martin *et al.*, 1998).

Work done = Force x Displacement [SI Unit: J; Derived Unit: $kg.m^2s^{-2}$]

$W = Fs$

(vi) Moment of Inertia

The moment of inertia, also defined as second moment area, is bone's ability to resist bending. It is calculated from the equation below.

$$I = \frac{\pi\left(d_E^4 - d_I^4\right)}{64}$$

d_E: External diameter

d_I: Internal diameter

(vii) Neutral Axis

When bone is bent, one side undergoes tension while the other side undergoes compression. The boundary between the two forces is where no stress is being exerted. This area is known as the neutral axis or neutral plane of the bone (Martin *et al.*, 1998).

1.5 Biomechanics of Blunt Force Trauma

Blunt force trauma (BFT) is one of the leading causes of mortality in homicidal cases globally. It can result from being struck by an implement, motor vehicle accidents, diseases, falls and natural disasters (Wedel and Galloway, 2013). While damage pertaining to violent attacks involving blunt force trauma tend to manifest itself more on the crania compared to the rest of the human skeleton, post-cranial damage is more evident in cases involving motor vehicle accidents and falls (Rastogi *et al.*, 1986; Lerer *et al.*, 1997; Ambade and Godbole, 2006; Thieme and Wingren, 2009; Matzopoulos *et al.*, 2015; Clark *et al.*, 2017). Studies focussing on blunt force trauma tend to be more skewed towards damages pertaining to the cranium (Sharkey *et al.*, 2011; Mole *et al.,* 2015). Hence, more research should be done on post-cranial damages to obtain a better injury profile involved in blunt force trauma. Post-cranial injuries often result in the production of wedge fractures, and a better understanding of their mechanism and propagation is thereby needed to better assist with

medicolegal investigations involving blunt force trauma (Rastogi *et al.*, 1986; Yukawa *et al.*, 1997; Davidson *et al.*, 2011).

As described in Section 1.2, blunt force trauma results from a low energy impact concentrated on a specific area on the bone. Blunt force trauma can vary from a simple crack to complete fragmentation of a bony structure with regards to the magnitude of impact energy and velocity (Kimmerle and Baraybar, 2008; Symes *et al.*, 2012; Kieser *et al.*, 2013; Cohen *et al.*, 2016). Upon impact, there is a transfer of kinetic energy to the skeletal element from the implement to the bone, resulting in elastic deformation. A crack will expand into complete failure should the stress factor at the crack initiation point exceed the bone's ability to resist stress (Wright and Hayes, 1976). This can further be explained as an excessive strain, resulting in a transition from bone's elastic phase into the plastic phase leading to failure as shown in Figure 1.8. The extent of deformation is dependent on the direction, rate and magnitude of loading (Currey, 2003a; Porta, 2005), while the type of impact (i.e., direct or indirect) affects the resulting fracture morphology. These will be discussed further at a later stage.

1.5.1 Factors Influencing the Biomechanics of Bone

Numerous variables influence blunt force injuries. These include, but are not restricted to, the size of the impactor's surface area, shape of object used, age and lifestyle of the victim (Kimmerle and Baraybar, 2008; Symes *et al.*, 2012). Intrinsic and extrinsic factors should be accounted for as they affect the propagation and extent of a fracture. Extrinsic factors can be defined as external variables acting on the body. These include impact force, velocity and energy and weapon shape as well as lifestyle factors such as drug use or alcohol intake. Intrinsic factors are defined as variables present in the body such as bone shape, density, strength and mineral composition (Hernandez and Keaveny, 2006; Symes *et al.*, 2012; Wedel and Galloway, 2013). The interplay between intrinsic and extrinsic forces provides a better understanding of bone's reaction to trauma.

(i) Intrinsic Factors

The mechanical properties and structural integrity of bone are dependent on numerous factors. Of main importance are age and pathological factors, as these result in an increased fracture risk (Wright and Hayes, 1976; Kress, 1996).

Bone strength and resilience are directly related to the proportion of lamellar bone and osteons. With increasing age, it has been suggested that there is a trade-off between the two, resulting in an increase in osteon numbers. This phenomenon results in an increase in the number of Haversian canals present in the bony structure, consequently causing a decrease in bone mass and density (Currey, 2003a; Wedel and Galloway, 2013). The resulting effect on the mechanical properties of bone include a 1.5% decrease in the elastic modulus of bone per decade, and a significant reduction in the ability to withstand stress before failure (5% - 7% decrease per decade) (Hipp and Hayes, 2013). Therefore, with increasing age, bone behaves in a more brittle manner rather than elastic.

Pathology is another factor which greatly affects the biomechanical properties of bone. Depending on the nature of the pathology, the plastic deformation phase of skeletal elements may either be increased or decreased. Turner (2002) discusses how osteopetrosis and osteomalacia affect bone's reaction to loading differently. From a purely biomechanical standpoint, osteopetrosis results in the hardening of bone tissue, leading to an increase in the stiffness and causes bone to behave in a more brittle way. Osteomalacia results in the softening of bone tissue, thereby causing bone to react in a more ductile and malleable way. Figure 1.10 depicts how pathology affects the biomechanical properties of bone during loading.

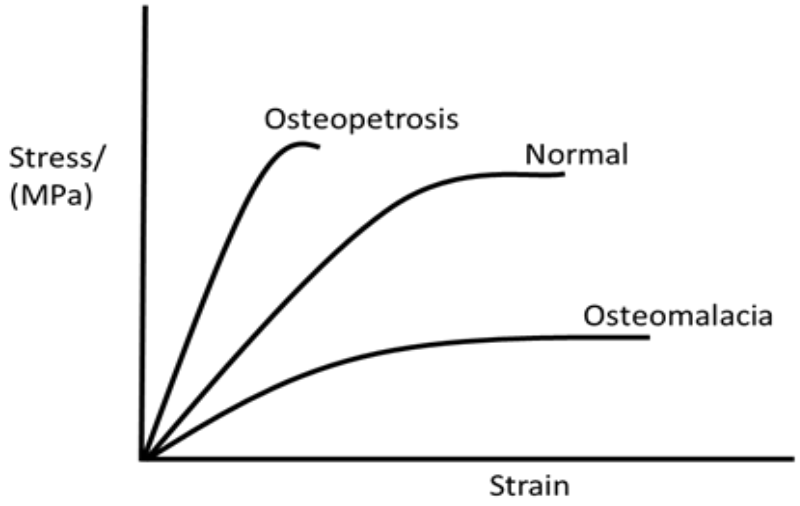

Figure 1.10

Force-Displacement Curves showing the effects of pathology on the response of bone when subjected to loading (Turner, 2002)

(ii) Extrinsic Factors

The understanding of fracture patterns and mechanisms is critical for anthropological reconstructions. Of importance are factors such as point of impact, the number and sequence of blows, the weapon used, and the amount of force and energy used during the insult (Symes *et al.*, 2012; Sharkey *et al.*, 2011; Mole *et al.*, 2015). A fracture may vary from a simple crack to complete fragmentation of the bony structure. It is understood that the crack will expand into failure should the stress factor at the crack initiation point exceeds the material's ability to resist stress (Wright and Hayes, 1976; Currey, 2003). Past literature has suggested that this can be attributed to loading force, type and direction, as well as geometry of the impact surface (Kress *et al.*, 1995; Reber and Simmons, 2015; Isa *et al.*, 2017).

1.6 Types of Long Bone Fractures

As explained in Section 1.4.1, when bone experiences loading, it will react in an elastic manner until yield point. Post-yielding, bone experiences irreversible damage eventually leading to failure as the stress applied exceeds the strength of the bone. Bone failure typically arises in the form of a fracture. Fractures can grossly be defined as a rupture in the continuity of bone tissue and may either be complete or incomplete. It has been suggested that bone failure may occur through at least one of three commonly known mechanisms. Firstly, a fracture may be produced as a result of a random event involving excessive force causing tissue failure through energy absorption and propagation. Secondly, weakening of bone tissue due to pathology (e.g., osteoporosis, menopause, metastatic tumour, congenital diseases, etc) and increasing age. Lastly, fractures may occur when a bone is exposed to repeated stress from either static or dynamic loading (Delahay and Sauer, 2007; Kieser *et al.*, 2013; Wedel and Galloway, 2013). Bones of the lower limbs are known for their load-bearing functions which makes them stronger in compression than in tension and shear. From this principle, the analysis of fractures may reveal information pertaining to the events that lead to trauma, timing of injury, force and direction of impact, loading mechanism and even the chronological order in which the blows were sustained (Sharkey *et al.*, 2011).

Gozna *et al.* (1982) classified four main types of long bone fractures (Figure 1.11) as described below:

(i) Transverse Fracture

A transverse fracture occurs when a long bone is exposed to a combination of both tensile and compressive forces. The side of impact of the skeletal element experiences compression while the surface opposite side of impact undergoes tension. Failure initiates on the side experiencing tensile forces and gradually propagates towards the compressive side. During this process, the outer layer of the cortex fails first, resulting in the exposure of the inner layer to maximum stress until failure. The fracture line propagates perpendicularly to the axis of the bone, creating a transverse fracture line. The main principle behind the formation of a transverse line is the existence of a neutral axis between the two areas experiences the opposite forces (i.e., tension and compression). As the crack moves from the tensile side, the neutral axis also moves from the centre of the bone towards the compression side.

(ii) Oblique Fracture

There are two suggested mechanisms that may result in an oblique fracture. In the first scenario, a long bone may be subjected to a combination of tension and compression, similar to the mechanism involved in the production of a transverse fracture, but with the compressive forces being higher in magnitude than the tensile forces. This causes the bone to fail in compression and results in the formation of an oblique fracture, running at a 45° angle to the axis of the bone. The second scenario consists of a combination of compressive and shear forces. The bone initially fails due to excess shear loading as the bone is twisting while compression pushes the bone down. This results in a transverse fracture being directed downwards from the point of failure while curling around the shaft of the bone.

(iii) Spiral Fracture

As mentioned in Section 1.4.1, a long bone subjected to a combination of tension and shear (torsion) forces often results in the production of a spiral fracture. Such fractures take the form of a spiral which runs along the longitudinal axis of the bone at a 40-45° angle, curving around the shaft. This mechanism creates a fracture with a vertical component and two sharp and pointed edges. However, it is yet to be confirmed as to

whether such fractures result as an initial failure in tension or in shear. Bertocci *et al*. (2017) have shown that less energy is required to produce spiral fractures compared to transverse and oblique fractures, but their study did not explore the full propagation of failure.

(iv) *Butterfly/Wedge Fracture*

Unlike other fracture patterns, a butterfly fracture involves axial loading along with compressive and tensile forces acting in a transverse plane during bending. The mechanism is similar to a transverse fracture with failure initiating in tension and progressing towards compression. However, because of the added axial loading, the maximum shear strength of the bone is exceeded. This causes the fracture to travel at a 45° angle with respect to the axis of the bone. Consequently, the fracture line splits into a Y- shaped pattern, resulting in the formation of a wedged-shaped segment.

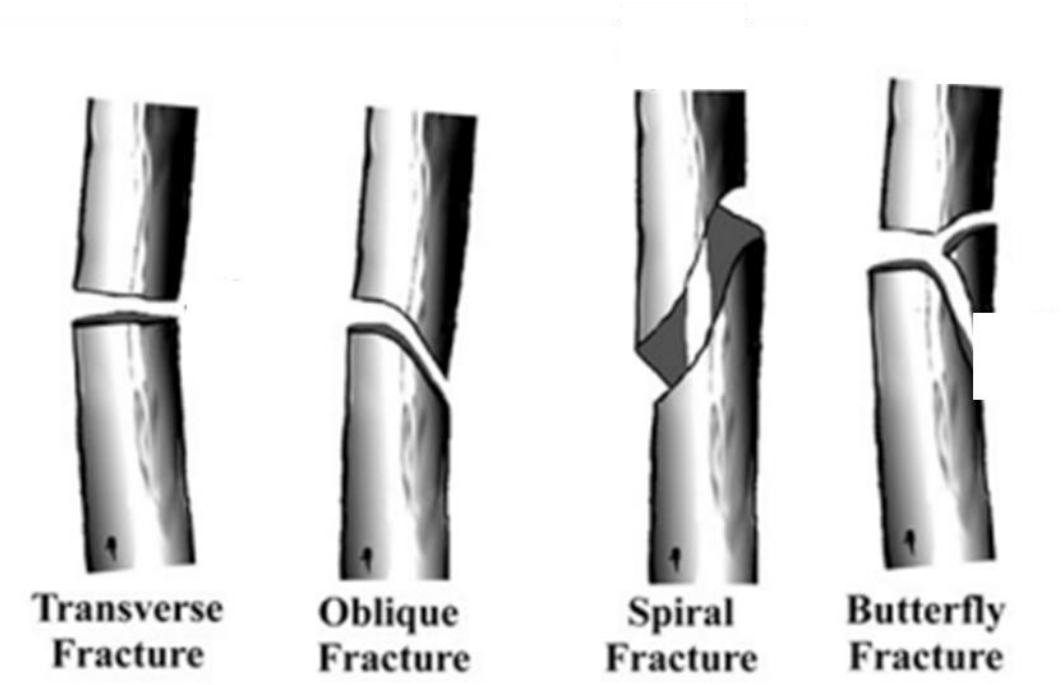

Figure 1.11

Diagrammatic representation of the different types of fracture patterns produced when long bones are subjected to blunt forces (Galloway and Zephro, 2005)

1.7 Formation and Interpretation of Wedge Fractures

The current method of interpreting the formation of wedge fractures dates from the 1880's. Recent studies have however, revealed a high degree of uncertainty in the reliability of this method, leading to erroneous reconstructions by forensic anthropologists (Reber and Simmons, 2015; Schmidt *et al.*, 2016; Isa *et al.*, 2017). The current study focusses on the formation and reconstruction of wedge fractures.

The wedge fracture, more commonly known as the butterfly fracture, is one of the most common injury patterns observed in long bone blunt trauma and was first described in 1880 by Otto Messerer (Messerer, 1880). He put forward a theory behind the mechanism of injury involved in the production of such fractures and proposed that it could be used to infer directionality of force and site of impact. Messerer suggested that butterfly fractures are a result of slow loading impacts involving a combination of tension and compression as a result of bending. The biomechanical explanation is that when a long bone is impacted perpendicular to the long axis at a low velocity, it will undergo bending, subjecting the impact side to compression and the opposite side to tension (Figure 1.12) (Khor *et al.*, 2006; Symes *et al.*, 2012). Given the fact that bone is weaker in tension than in compression, cortical failure initiates on the opposite side of the impact site (tension) and the crack travels to the site of impact (compression). As this occurs, shear stresses exceed the shear strength of the bone, causing the fracture line to split into two. This results in a Y-shaped pattern with a triangular breakaway fragment defined as the butterfly (Messerer, 1880; Passalacqua and Fenton, 2012; Reber and Simmons, 2015).

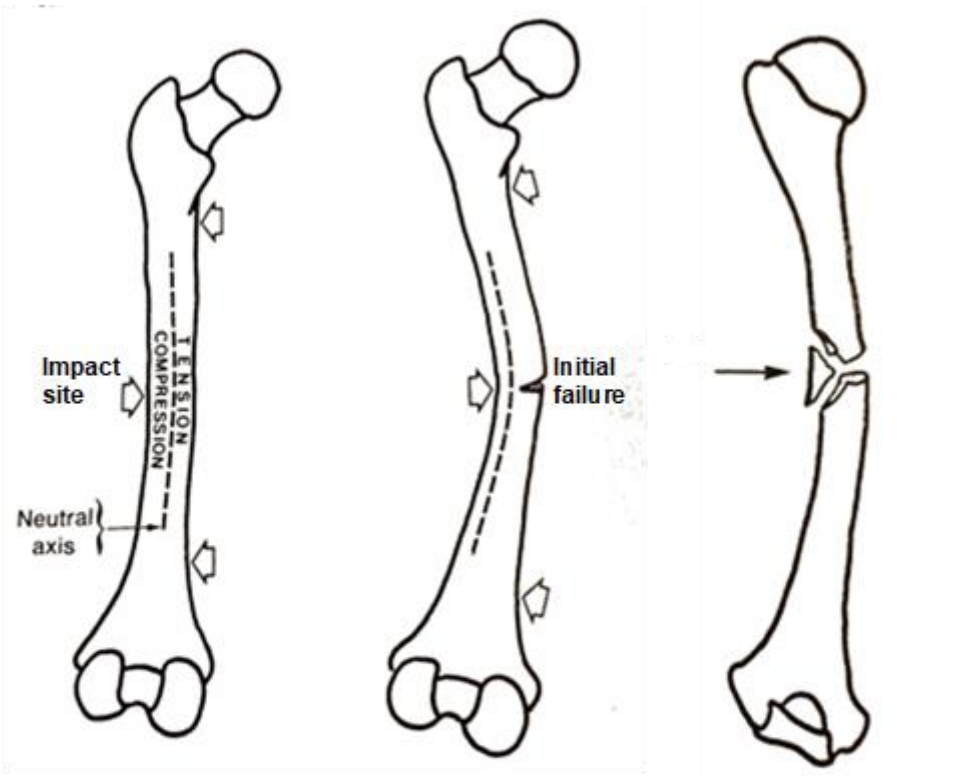

Figure 1.12

Schematic representation of the production of a wedge fracture when bone is subjected to tension and compression during bending (Gozna et al.,1982).

Forensic anthropologists make use of the Messerer theory in their anthropological reconstructions and use the wedge fragment to infer directionality and site of impact. The assumption is that the base of the triangular wedge is from the impact side, while the apex is from the site of initial failure (Messerer, 1880; Symes *et al.*, 2012; Reber and Simmons, 2015; Isa *et al.*, 2017). Thus, the apex points in the same direction that the force was applied. While this principle is being widely used in the medicolegal reconstructions involving blunt trauma to long bones, it has been shown that wedges may be produced with initial failure happening on the side undergoing compression (Rabl *et al.*, 1996; Teresinski and Madro, 1999; Reber and Simmons, 2015; Schmidt *et al.*, 2016).

The experiment performed by DeLand (2013) confirmed the biomechanical theory of crack bifurcation which states that when bone is loaded transversely at rates exceeding its load-bearing strength, failure will result in crack bifurcation causing two fracture lines to travel diagonally away from site of initial failure. The author further

suggests that the curving of the fracture lines at a 45° angle is influenced by the pattern of osteon distribution within cortical bone along the parallel axis. Mechanical tests have shown that osteon alignment causes fracture toughness of cortical bone to be lower along its longitudinal axis. This is further explained by the “mirror” zone theory, which suggests that a fracture will travel linearly at constant speed until a reflection boundary is reached (Ravi-Chandar and Knauss, 1984). This results in crack branching, causing the split lines to travel through the void areas found in between osteons. A common behaviour of the split fractures is to curve and travel diagonally.

Studies focussing on the production of wedge fractures have reported the occurrence of “false” or “reversed” wedges, which contradicts the current ideology that prevails in forensic anthropology with regards to the mechanism of injury of the butterfly fragment. This suggests that contrary to popular belief, failure may initiate on the side experiencing compression (side of impact), with fracture lines travelling to the side experiencing tension, resulting in the production of a butterfly breakaway fragment. Additionally, it raises issues about the accuracy of inferring directionality and site of impact from wedge fragments (Kress *et al.*, 1995; Delahay and Sauer, 2007; Thomas, 2011; Reber and Simmons, 2015).

For the sake of clarity, the wedge described by Messerer shall henceforth be defined as a tension wedge and a fragment produced from initial compressive failure shall be referred to as a compression wedge, as depicted in Figure 1.13.

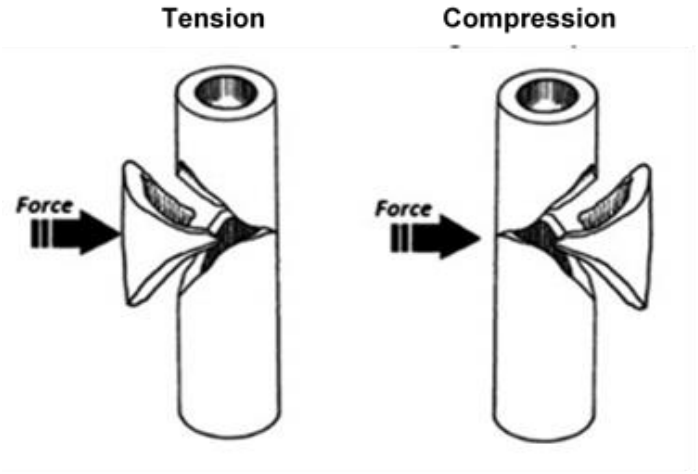

Figure 1.13

Diagrammatic representation of a tension wedge (left), with initial failure occurring in tension and a compression wedge (right), with initial failure occurring in compression (Reber and Simmons, 2015).

It has previously been noted that the nature of the wedge fracture (i.e., either tension or compression) is dependent on the anatomical impact side and the geometry of the bone (Kress, 1996; Reber and Simmons, 2015; Cohen *et al.*, 2016; Isa *et al.*, 2017).

Kress (1996) performed a study documenting the different fracture patterns that are produced when long bones are subjected to low velocity impacts. The specimens used consisted of embalmed human femora, which were either impacted anteroposteriorly or lateromedially. The first set up of the study consisted of an accelerator which pushed a wheeled cart towards the specimen at an approximate velocity of 7.5 m/s. Of the 32 femora which were impacted anteroposteriorly, 3.1% showed tension wedges and 6.3% showed compression wedges. The remaining fractures were split between comminuted, oblique, side wedge and segmental. The second sample, impacted lateromedially by a swinging pipe, consisted of 18 femora, of which 16.7% showed tension wedges and 11.1% showed compression wedges. The remaining fractures consisted of segmental, oblique, comminuted and other wedges. Kress (1996) concluded that impact side plays a significant role in the production of wedge fractures. He proposed that given bone is non-homogenous and anisotropic, along with being load-bearing, it is stronger and more resistant when impacted anteroposteriorly compared to lateromedially.

Isa *et al.* (2017) studied the mechanism of injury behind the production of wedge fractures. Their sample set consisted of 13 fresh unembalmed human femora which were impacted transversely using a 3-point bending fixture mounted on a servohydraulic material testing machine. An axial load of 450N was applied to the bone to mimic the load bearing function of the human leg. Six femora were impacted on the anterior side (A-P) and the remaining seven were impacted on the posterior side (P-A). All 13 femora were fractured, however, none produced a complete wedge fracture. Energy required for failure ranged from 15.0 to 66.3 J, where posterior impacts required more energy (39.4 ±18.4 J) than anterior impacts (29.0 ± 11.7 J) to cause fracture. Incomplete wedge fractures were present in 84.6% (11 of 13 femora) of the samples, which included 100% (6 of 6) of the A-P impacts and 71.4% (5 of 7) of the P-A impacts. The remaining 15.4% were either transverse or oblique fractures.

Studies have also been conducted on animal bone as a proxy for human tissue. Reber and Simmons (2015) utilised 255 sheep femora to investigate the mechanism of injury associated with the production of wedge fractures along with the reliability of inferring directionality from them. Specimens were divided into anterior and posterior impact tests. The bones were struck using either a pendulum apparatus or a drop test designed to stimulate 3-point bending from bumper impacts in pedestrian road accidents. Their results showed that 90% of their sample set was fractured, of which 49% produced complete wedge fractures. Of the complete wedge fractures, 60% were tension wedges and 40% were compression wedges. Furthermore, their experiment showed that anatomical impact side and bone geometry affected the production of wedge fractures. Anterior impacts were 69.7 times more likely to produce a butterfly fracture rather than a non-butterfly fracture, while posterior impacts were 151.9 times more likely to produce a non-butterfly fracture. Anatomical impact side and bone geometry also played a role in the production of tension and compression wedges. Anterior impacts were 1.7 times more likely to produce a tension wedge, while posterior impacts were 5.7 times more likely to produce a tension wedge. The assessment of directionality inference using the current methodology (i.e., Messerer's theory) could only be applied to 49% of the whole fractured sample set as it required the presence of a detached wedge piece. Of the 49% assessed, the method was only 60% accurate. These results indicate a need for further research into the production and propagation of wedge fractures.

The two aforementioned studies (Reber and Simmons, 2015; Isa *et al.*, 2017) reported that impact force and energy had no statistical significance on the nature of the wedge fracture produced (i.e., tension wedge vs compression wedge). Of significant importance were impact side (i.e., anterior vs posterior) and bone geometry. Isa *et al.* (2017) reported that 100% of the femora impacted anteriorly and 71.4% of those impacted posteriorly resulted in failure on the tensile side. Reber and Simmons (2015) reported that anterior loading was 69.7 times more likely to produce a wedge fracture while posterior loading was 151.9 times more likely to not result in one. Of the impacts that resulted in wedge fractures, anterior loading and posterior loading were 1.7 times and 5.7 times more likely to result in a tension wedge. In terms of inferring directionality, Isa *et al.* (2017) suggested that the full fracture morphology should be assessed given not all cases result in the production of a complete detached wedge

fragment. This was also supported by Reber and Simmons (2015) who further suggest an analysis of the wedge angle to refine the method used for inferring directionality up to 98% accuracy. Their results showed that tension wedges tend to have acute apices while compression wedge tend to have obtuse apices.

Deducing side of tension and side of compression can further be refined by the analysis of microscopic surface features. Isa *et al.* (2017) noticed that the tension surfaces of their fractured specimens were flat, with shallow billowing. The compression surfaces, on the other hand, were jagged, with a steep profile. These characteristics are in agreement with the observations of Symes *et al.* (2012) and Scheirs *et al.* (2017). The general consensus is that tension surfaces are flat and billowy as they experience tearing while compression surfaces are jagged, with step breakage, break away spurs and microfractures due to being crushed.

Scrutinisation of the existing pool of literature surrounding the biomechanics of butterfly fractures has showed that our current understanding of the fracture pattern is skewed. While studies performed by Martens *et al.* (1986) and Khalil *et al.* (2015) have resulted in the production of tension wedges only, thereby complying with the assumption that all butterfly fractures are a result of bone failing in tension, other studies have demonstrated otherwise. Thomas and Simmons (2011), along with Rabl *et al.* (1996) and Kress *et al.* (1995), have demonstrated the occurrence of compression wedges when long bones are subjected to bending impacts. Furthermore, the importance of acknowledging incomplete butterfly fracture patterns in forensic analyses has been brought forwards by Fenton *et al.* (2012) and DeLand (2013). Altogether, the results produced by these authors (Table 1.1) further concretise the variability present in the production of wedge fractures and therefore, highlights the importance of investigating the fracture mechanisms associated with long bones during bending impacts so as to better the existing methods of analysis pertaining to butterfly fractures.

***Table 1.1**: Summary of studies investigating the production of tension and compression wedges in lower limb bones, and the energy required to initiate the fracturing of long bones.*

Study	Specimen	Test Apparatus	Fracture Energy/ J	Wedge fracture production
Bertocci *et al.* (2017)	Porcine femora	Servohydraulic Testing Machine	2.92	No wedge fractures; transverse, oblique and spiral
Cohen *et al.* (2016)	Porcine	Pendulum Machine	20.6- 60.4	1 compression wedge recorded
DeLand (2013)	Human femora	Servohydraulic Testing Machine	14.96 – 66.30	42.7% incomplete tension wedge
Dempsey *et al.* (2018)	Sheep tibias	Drop Test	90-135	No wedge fractures; shattering of bone
Fenton *et al.* (2012)	Human femora	Servohydraulic Testing Machine	-	80% incomplete tension wedges No compression wedges
Isa *et al.* (2017)	Human femora	Servohydraulic Testing Machine	15 – 66.3	84.6% incomplete tension wedges
Khalil *et al.* (2015)	Sawbones© Model tibias	Dynamic 3 Point-Bending Impactor	-	100% complete tension wedges
Kress (1996)	Human femora	Wheel Cart Accelerator	-	6.3% complete compression wedges 3.1% complete tension wedges

	Human Femora	Swinging Pipe		16.7% complete tension wedges 11.1% complete compression wedges
Kress *et al.* (1995)	Human femora	Wheel Cart Accelerator	-	24% complete tension wedge 4% complete compression wedge
	Human tibias	Wheel Cart Accelerator	-	21.1% complete tension wedge 4.2% complete compression wedge
Martens *et al.* (1986)	Human femora	Servohydraulic Testing Machine	36.8	Tension wedges
Rabl *et al.* (1996)	Human tibias	Servohydraulic Testing Machine	-	65.6% complete tension wedge 34.4% complete compression wedge
Reber and Simmons (2015)	Sheep femora	Pendulum and Drop Test	-	60% tension wedges 40% compression wedges
Scheirs *et al.* (2017)	Autopsy cases Wet human long bones Dry human	Servohydraulic Testing Machine	82.9-118.4	~15% ~28% ~9% } No distinctions were made between tension and compression wedges
Thomas and Simmons (2011)	Sheep femora	Drop Test	-	Both tension and compression wedges present Percentages not reported
Teresinski and Madro (1999)	Car-Pedestrian Collision	Case Reports		
	Tibias	-		82.1% complete tension wedge 3.5% complete compression wedge
	Femora	-		50% complete tension wedge 21.4% complete compression wedge

1.7.1 Concluding Remarks on the Production and Interpretation of Wedge Fractures

The aim of this review was to investigate the production and interpretation of wedge fractures with regards to previous literature. As indicated, the biomechanics involved behind the formation of wedge fractures are not as clear as previously thought. Although tension wedges are comparatively more common, the occurrence of compression wedges needs to be acknowledged as it further accentuates the issue of dogmatically making use of Messerer's theory when inferring directionality in medicolegal reconstructions. Furthermore, previous studies have also demonstrated the presence of incomplete butterfly fracture patterns and it is imperative that enhanced investigations be performed to refine forensic reconstructions. It is therefore evident that further research is required to ascertain the conditions under which tension and compression wedges are produced in order to accurately assist with the reconstruction of mechanism of injury and inference of impact directionality during medicolegal investigations involving blunt force trauma.

2. METHODOLOGY

The purpose of the study was to investigate the mechanism of injury of wedge fractures when a long bone is subjected to blunt force trauma resulting in bending. The study was conducted with two objectives.

(i) The primary objective was to document the production of wedge fractures during 3-point bending impacts using sheep femora.

(ii) The second objective was to test the reliability of the current method of inferring directionality from wedge fractures, as well as the updated methods proposed by Reber and Simmons (2015).

2.1 Rig Construction

A drop rig was built to simulate blunt force impacts. The work was undertaken at the University of Cape Town. The impact rig consisted of a steel frame, a weighted impactor (also referred to as a gravitational accelerated mass, GAM), metal cables for increased stability and a wooden adjustable bone stand (Figure 2.1). The total rig measured 2.5 m in height to allow for testing at different drop heights and had a 1.5 m x 1.5 m square base. The weighted impactor was designed to easily enable the addition or removal of weights, thus altering the potential impact energy. The impacting surface was a hollow steel pipe with an external diameter of 35.72 mm and an internal diameter of 23.94 mm.

The bone stand was designed to allow for 3-point bending of bone specimens. During testing, bone specimens were positioned horizontally within the wooden bone stand to ensure perpendicular impact to the desired location on the bone (Figure 2.2). The specimen was mounted at least 20 cm above ground level to allow the bone to bend freely during impact. This ensured that any fractures produced were as a result of pure bending and not torsional stress and/or subsequent crushing against a surface.

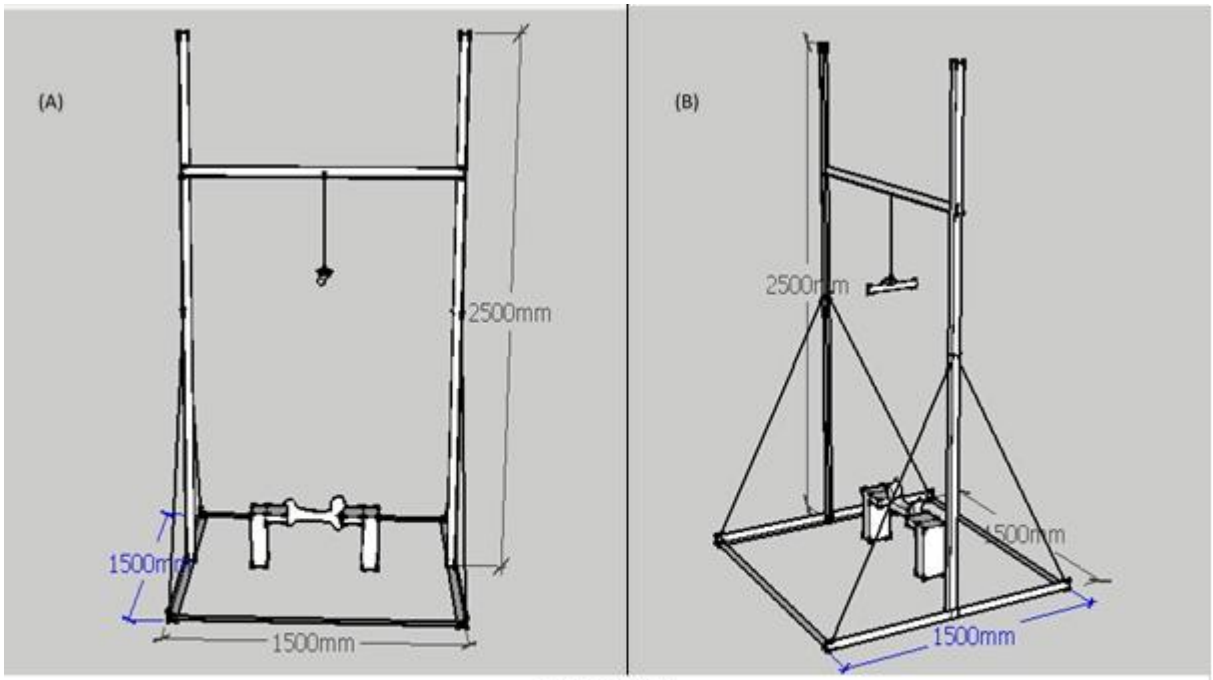

Figure 2.1

Diagrammatical representation of the impact rig. **(A)** Anterior view **(B)** Anterolateral (overall) view (Images created with Sketch Up Pro, [Google, 2016])

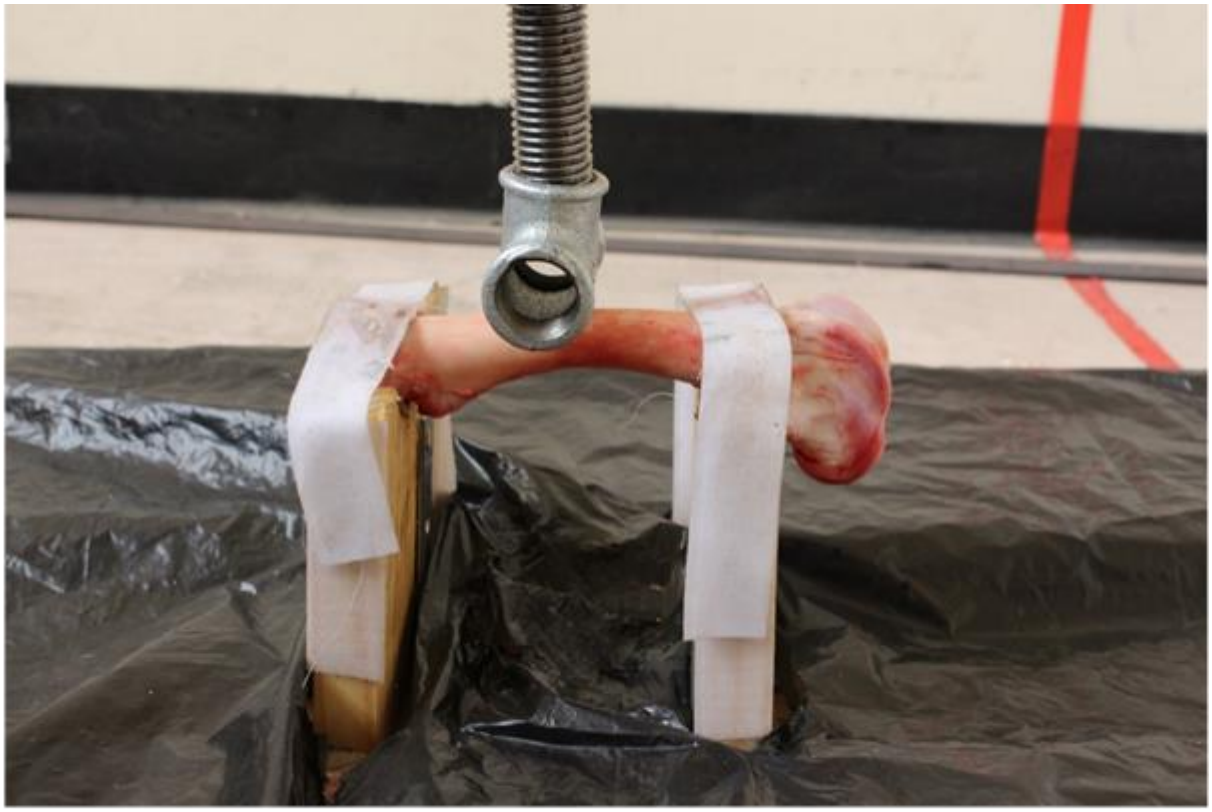

Figure 2.2
Lateral view of impact

2.2 Specimen Preparation

A total of forty sheep (*Ovis aries*) femora were obtained from local abattoirs for the study. Bones were obtained mostly cleaned with some soft tissue and periosteum remaining intact. Ethical clearance for the use of animal tissue was granted by the Animal Ethics Committee of the University of Cape Town (ref: AEC 018_044).

A number of different specimens have been used to conduct such research in the past, including human (Martens *et al.*, 1986; Kress *et al.*, 1995; Isa *et al.*, 2017), bovine (Cooke *et al.*, 1973; Wright and Hayes, 1976) , porcine (Bertocci *et al.*, 2017; Cohen *et al.*, 2017) and ovine (Thomas and Simmons, 2011; Reber and Simmons, 2015; Dempsey *et al.*, 2018). Due to ethical considerations it is not always possible to obtain or utilise human tissue for research, as such it is necessary to determine suitable surrogates for such research. The current study used sheep femora as a proxy for human bones. Contrary to bovine and porcine bones, sheep bones are a better substitute as they are closer to human bones in terms of geometry and toughness (Thomas and Simmons, 2011; Reber and Simmons, 2015; Dempsey *et al.*, 2018). The energy required to fracture sheep and human bones have an overlapping range, while porcine bones are fractured at energies below the minimum energy required to fracture human bones (Martens *et al.*, 1986; Bertocci *et al.*, 2017). No energies have been reported for impact studies performed on bovine bones.

Furthermore, given that the aim of this study is to assess the reliability of inferring directionality from wedge fractures, the importance of comparing with Reber and Simmons (2015) should be stressed.

The bones were collected in a frozen state and kept at -4°C until testing. Prior to testing the bones were allowed to thaw for approximately 24 hours. It has been put forward that freezing and thawing of bones do not affect the biomechanics involved during fracture, although care should be taken that the bones are fully thawed before impact (Torimitsu *et al.*, 2014).

Any soft tissue remaining on the diaphysis was carefully removed away by dissection. This was done to ensure accurate anatomical orientation of the bone during the experiment. After dissection, the bones were visually analysed for pathology and/or

any damage which could interfere with the integrity of the specimen. Bones which were affected were not included in the experiment.

Post-impact, the marrow was carefully removed out of the fractured bones with the use of scalpels and tweezers. Data collection such as measurements and fracture pattern recording was then performed (discussed further below).

2.3 Testing and Data Recording

Three-point dynamic bending tests were performed using the drop apparatus described in Section 2.1. Specimens were subjected to single impact tests to the mid diaphysis under two different energy conditions calculated using the following equation:

Potential Energy = mgh

[m = mass (kg); g = acceleration (ms^{-2}); h = height (m)]

The first condition was generated by dropping a weight of 2.3kg from a height of 1m, resulting in 22.6J of energy. The second condition was generated by dropping a 3.3kg weight from a height of 1.5m, resulting in 48.56J of energy. Specimens were further divided into two subgroups based on the orientation of impact, either impact to the anterior or posterior aspect of the femur. This resulted in 10 specimens within each impact group (Figure 2.3).

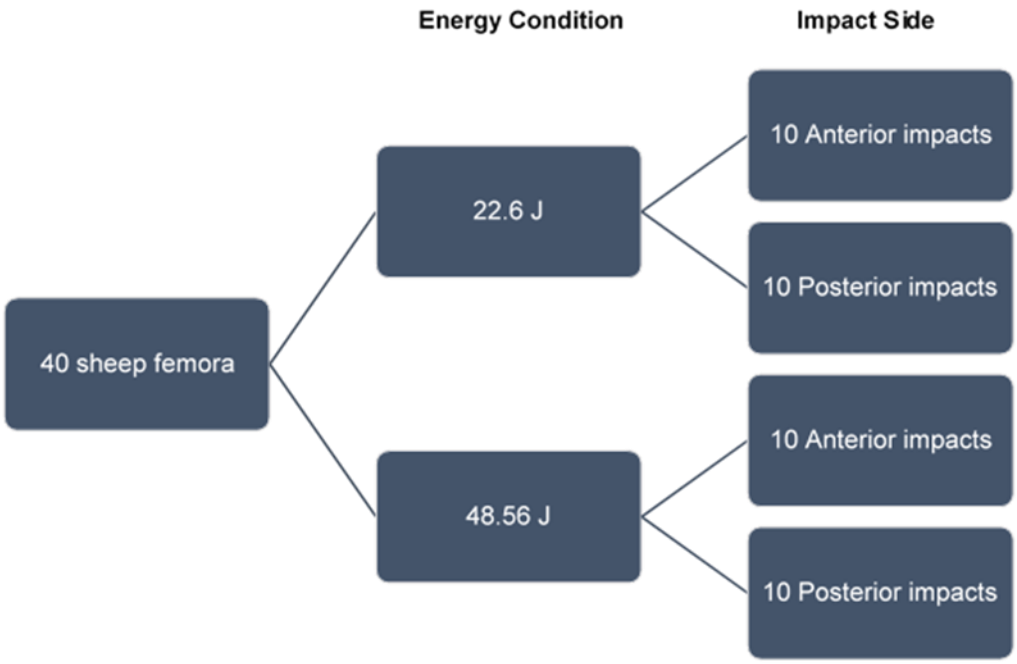

Figure 2.3
Distribution of femora according to energy condition and side of impact

2.4 Data Collection

Prior to impact, numerical parameters such as length, external anteroposterior and mediolateral diameters were recorded. After impact, anterior, posterior, lateral and medial thicknesses were measured along with internal anteroposterior and mediolateral diameters. Bone length was measured by using a standard ruler. All other measurements were taken with the use of Vernier callipers. Bones which did not break during impact were sawed to have the internal measurements taken. Figure 2.4 depicts the measurements taken.

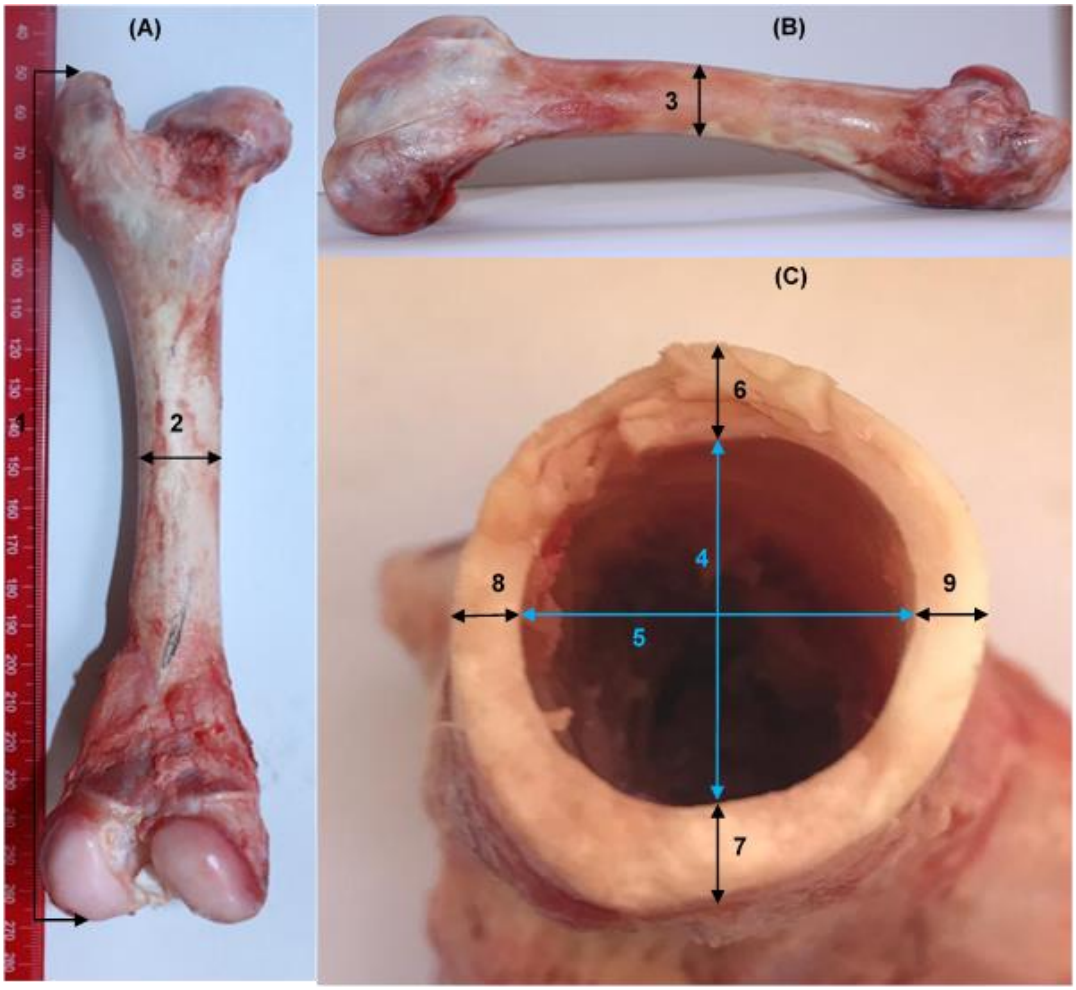

Figure 2.4

*Measurements taken prior and post impact. **1)** Total Length, **2)** External Mediolateral Diameter, **3)** External Anteroposterior Diameter, **4)** Internal Anteroposterior Diameter, **5)** Internal Mediolateral Diameter, **6)** Anterior Cortex Thickness, **7)** Posterior Cortex Thickness, **8)** Medial Cortex Thickness, **9)** Lateral Cortex Thickness.*

Post-impact, the specimens were classified as “fractured” or “not-fractured”, after which fracture patterns from the fractured bones were analysed visually and recorded. Fracture patterns were classified as wedge (complete/partial), lunate (complete/partial), transverse, linear, comminuted or a combination thereof. The fracture surface of each bone was further analysed and morphologically described visually to determine compressive and tensile surfaces. Other fracture pattern descriptions included extreme shatter and missing point of impact.

2.5 Data Analysis

Statistical analyses were performed using Stata 13 software (StataCorp, Tx, USA). Logistic regressions were performed for each parameter to determine which variable was the most significant in the production of *(i) fractures and (ii) complete butterfly type fractures*. The variables taken into consideration were *(i) Energy, (ii) Moment of Inertia, (iii) Cortical Thickness and (iv) Side of Impact.*

Fisher's Exact tests were performed to investigate:

(i) whether side of impact influenced the production of butterfly fractures within particular energy group

(ii) whether energy influenced the production of butterfly fractures within a particular impact side group.

Standard t-tests were performed to assess whether any differences in the means of variables for the two impact groups were of significance.

Accuracy of inferring directionality from butterfly fracture patterns was measured by applying three techniques. The first technique tested assumed that the apex of the triangular wedge pertained to the site of initial failure (tension) while the base pertained to side of impact (compression). The second method tested was the one put forward by Reber and Simmons (2015), stating that compression wedges have an obtuse apex (lunate) while tension wedges have an acute apex (wedge). The third method consisted of visually analysing the overall fracture morphology.

3. RESULTS

3.1 Fracture Production

Three point bending impacts were conducted on 40 sheep femora, which were randomly separated into two impact energy groups.. Each energy group was further sub-divided into anterior impacts and posterior impacts. Table 3.1 shows a summary of the means of the numerical parameters measured for each energy group.

Table 3.1: *Summary of mean parameters measured in each femur and p-values for mean differences*

Parameters	22.6 J	48.56 J	p-value
Cortical thickness	145.4	194.1	0.99
Length	186.1	186.7	0.875
Moment of Inertia	6243.9	6284.8	0.968

Of the 40 femora, 85% (34/40) were fractured, with 20 bones exhibiting butterfly fracture patterns, either complete, partial or a combination thereof. Other fracture patterns produced during the experiment included transverse fractures (52.94%), linear fractures (8.82%) and comminuted fractures (35.29%). Except for transverse fractures, which sometimes occurred in isolation, all the other fracture patterns occurred as a combination of two or more types. Figure 3.1 summarises the percentage of fractured bones and fracture patterns.

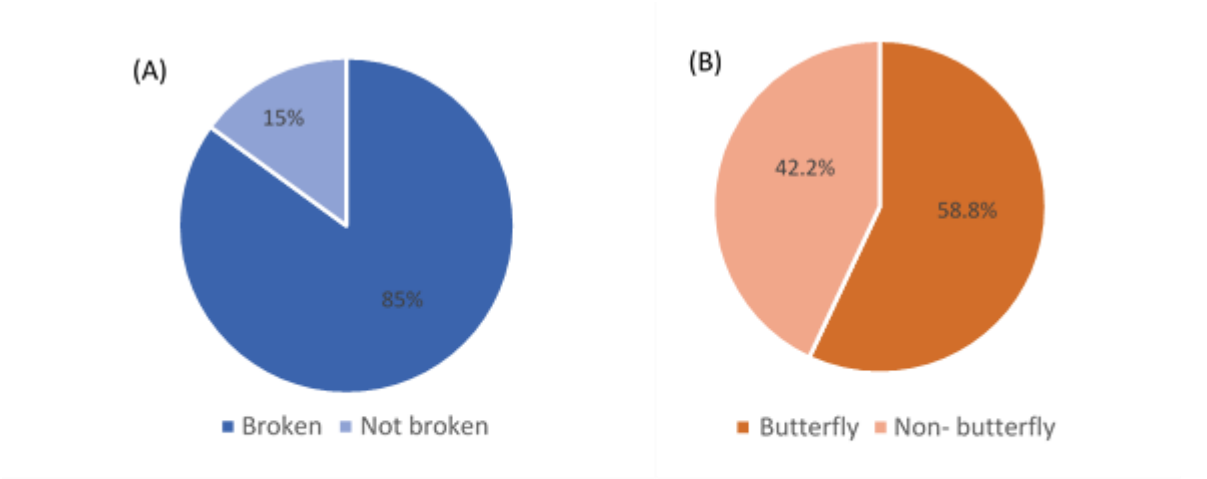

Figure 3.1: Summary distributions of fractures

(A) Summary of total bones broken during impact tests.

(B) Distribution of overall fracture patterns.

Logistic regression was performed for each individual variable to assess their respective significance levels in the fracturing of the femora. The variables investigated were energy, side of impact, cortical thickness and moment of inertia. Table 3.2 below summarises the respective results obtained for each regression run.

Table 3.2: *Logistic regression models assessing odds of fracture*

Variables	p-value	Pseudo R^2	X^2 probability	Odds Ratio
Energy	0.455	0.017	0.445	1.993
Side of Impact	0.133	0.085	0.087	0.179
Cortical Thickness	0.108	0.075	0.109	0.999
Moment of Inertia	0.351	0.024	0.366	1.000

The models showed that while none of the investigated variables significantly accounted for the fracturing of the sheep femora upon impact, a weak association can be inferred for cortical thickness and side of impact. When interpreting the pseudo R^2 values in congruence with each other, side of impact stands out as the variable responsible for predicting the variability of the results, followed by cortical thickness, moment of inertia and lastly energy. From the odds ratios, it can be inferred that an

increase in energy will have the highest influence on the fracturing of the bones, with regards to the other variables. Furthermore, it can be postulated that anterior impacts are more likely to result in a fracture, compared to posterior impacts. Nonetheless, the results generated should be interpreted with caution given the low pseudo R^2 and high X^2 probability values, both of which predict the robustness of the models used.

3.2 Butterfly Fracture Patterns

Twenty bones showed butterfly fracture patterns, either complete, partial or a combination thereof, after being impacted. Eight of the 20 (40%) femora produced detached butterfly pieces. Of the femora which showed butterfly fractures, 62.5% were those which were impacted at 22.6 J. These impacts produced two complete wedges, two complete lunates, one partial wedge and two partial lunates when impacted anteriorly. When impacted posteriorly at the same energy, the butterfly fracture patterns produced were one complete wedge, one complete lunate, two partial wedges and two partial lunates. The remaining 37.5% of femora displaying butterfly type fractures were those impacted at 48.56 J. Anterior impacts under this condition resulted in one complete wedge, two complete lunates, two partial wedges and two partial lunates, while posterior impacts only resulted in three partial wedges. Figure 3.2 shows the percentages of butterfly fracture patterns which occurred during the impact tests and Figure 3.3 depicts the morphology of each butterfly fracture pattern.

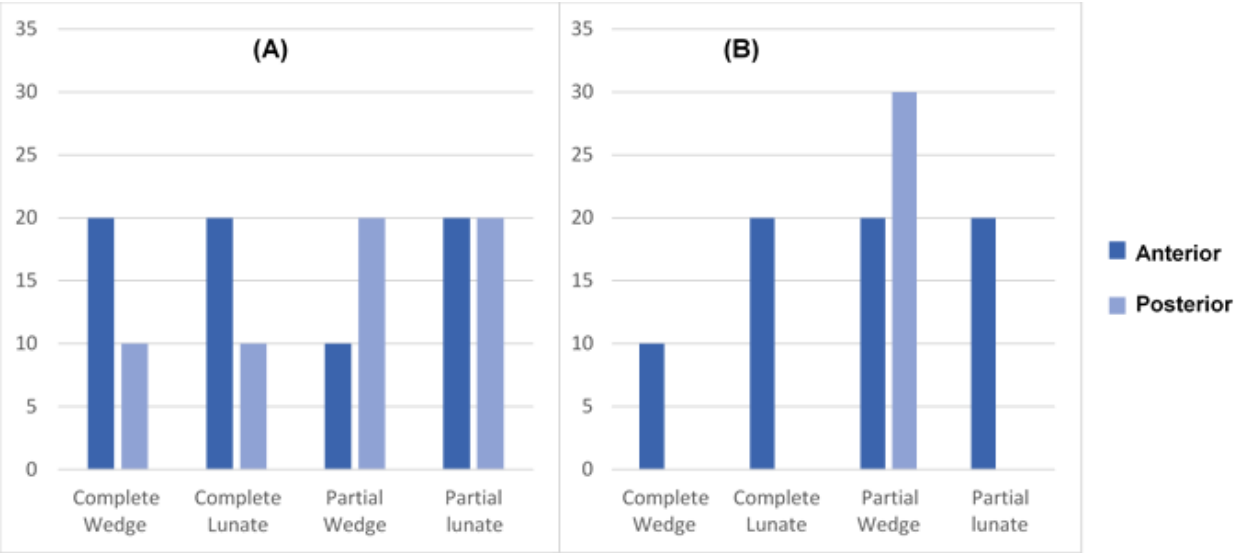

Figure 3.2

Butterfly fracture distribution, both complete and partial during impacts.

***(A)** summarises impacts at 22.6 J; **(B)** summarises impacts at 48.56 J.*

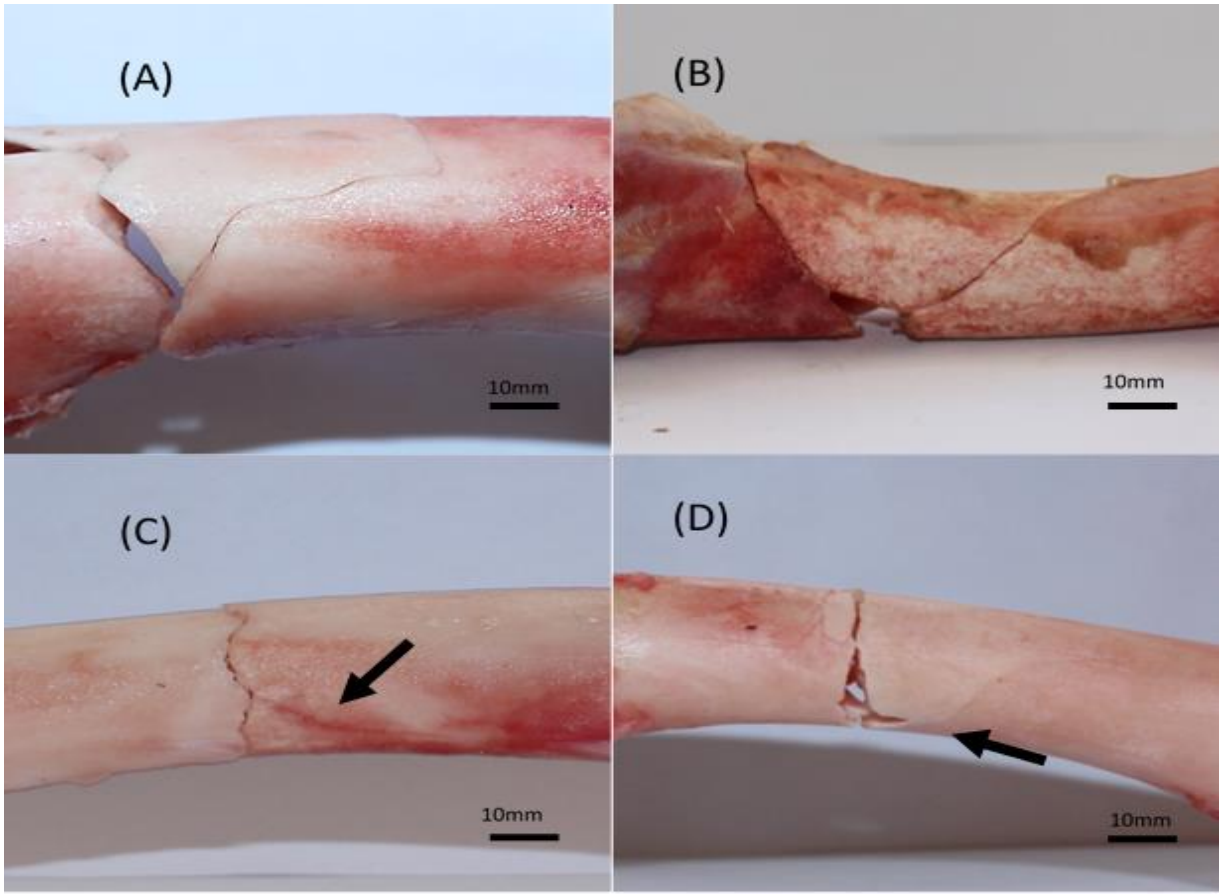

Figure 3.3 Butterfly type fractures produced during testing

***(A)** shows a complete wedge fracture, **(B)** shows a complete lunate fracture, **(C)** shows a transverse with partial wedge fracture and **(D)** shows a transverse with partial lunate fracture. Arrows point to partial fractures.*

Fisher's exact test was performed for each energy group to investigate whether side of impact played a significant role in the production of butterfly fractures. Both the 22.6J impact and 48.56 J impact groups showed that side of impact was not of significance (*p=0.820 and 0.179, respectively).*

A similar test was then performed to investigate whether impact energy influenced the production of butterfly fracture patterns within a particular side of impact group. No significant association was noted between impact energy and production of butterfly fractures within both the anterior and posterior impact (*p=0.675 and 0.370, respectively).*

Individual logistic regressions were performed for each variable to assess their respective significance levels in the production of complete butterfly fracture patterns. Table 3.3 depicts the results for each model.

Table 3.3: *Logistic regression models assessing odds of complete butterfly fracture production*

Variables	p-value	Pseudo R^2	X^2 probability	Odds Ratio
Energy	0.210	0.036	0.195	0.378
Side of Impact	0.059	0.092	0.039	5.143
Cortical Thickness	0.034	0.156	0.007	0.974
Moment of Inertia	0.941	0.049	0.132	1.071

Cortical thickness showed the highest level of significance with regards to the other variables, followed by side of impact. The low chi-square probabilities and relatively high pseudo R^2 values confirm the reliability and robustness of both respective models. Assessment of the odds ratio reveal that anterior impacts are 5.143 times more likely to result in butterfly fractures compared to posterior impacts. The odds ratio generated for cortical thickness predict that an increase in the variable would result in lower chances of producing a butterfly fracture. The difference in cortical thickness for the two impact groups was not significant (*p=0.99*), thus this result is unlikely to be as a result of randomisation into the different energy groups. The results generated for moment of inertia and energy revealed that these two variables do not play a significant role in the production of butterfly fractures.

3.3 Interpreting Directionality

From the impacts, a total of nine complete butterfly pieces were obtained along with fourteen partial fractures. Table 3.4 summarises the distribution of the four different fracture patterns between anterior and posterior impacts.

***Table 3.4**: Distribution of butterfly fractures according to side of impact*

Morphology	Anterior	Posterior
Wedge	3	1
Lunate	4	1
Partial wedge	3	5
Partial lunate	4	2

***Table 3.5**: Distribution of butterfly fractures with regards to direction of apex*

Morphology	Same Side as Impact	Opposite Side of Impact
Wedge	1	3
Lunate	3	2
Partial wedge	0	8
Partial lunate	6	0

The totality of fracture patterns facing either side of impact or opposite can be seen in Table 3.5. Upon analysis, it was revealed that lunate type fractures can be present on the side experiencing tension (opposite side of impact) and similarly, wedges can be found on side experiencing compression (side of impact). Figure 3.4 depicts one example for each scenario. This highlighted the flaws when applying the existing methods of inferring directionality from butterfly fractures, as summarised in table 3.6.

***Table 3.6**: Applicability and accuracy of existing methods*

Method	Applicability (%)	Accuracy (%) (butterfly fracture sample)	Overall Accuracy (%) (fractured sample)
Messerer's Method (Otto, 1880)	26.5	22	5.9
Fragment Angle (Reber and Simmons, 2015)	26.5	66.7	17.6
Overall fracture morphology (Reber and Simmons, 2015)	67.6	87	59

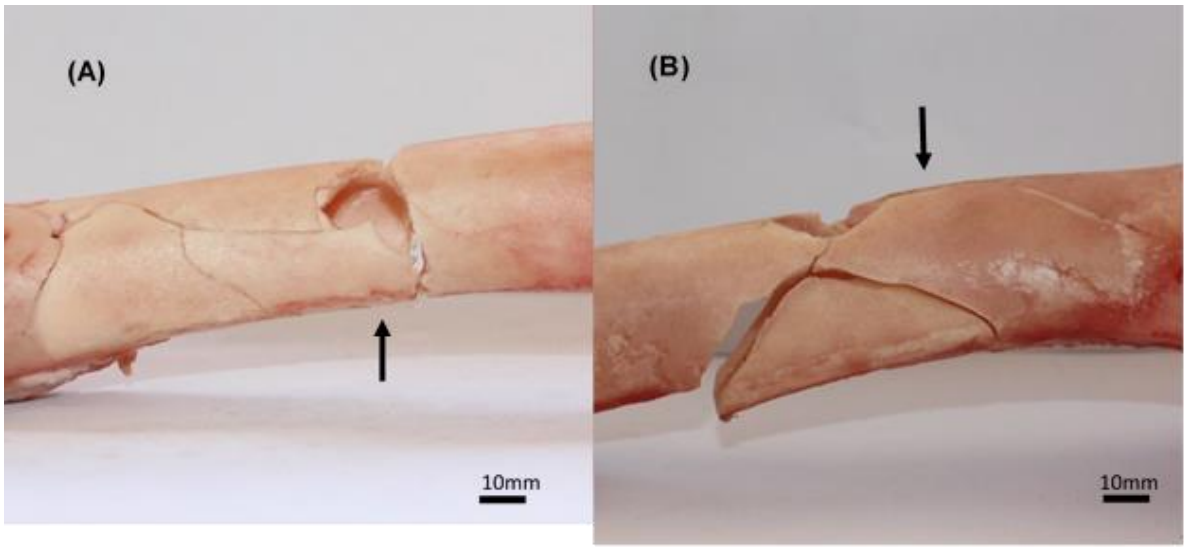

Figure 3.4

***(A)** shows a compression fracture occurring opposite side of impact.*

***(B)** shows a wedge fracture occurring on side of impact. Arrows depict side of impact.*

3.4 Surface Characteristics

One noteworthy observation made during the visual assessment of the fractured bones was surface characteristic. Clearly visible discrepancies were noted between tension and compression points. Tension surfaces were smooth, showing evidence of tearing, while compression surfaces exhibited characteristics such as layered breaks, crushed margins and flaking. All fractured bones (100%) showed evidence of tension surface characteristics, while compression surface characteristics varied. Layered breaks (67.7%), often occurring in isolation, were almost always present in bones which produced a transverse fracture upon impact. Crushed margins and flaking

always occurred as a combination and were present in impacts which resulted in extreme shatter (32.3%). Figure 3.5 depicts the difference between compression and tension surface characteristics.

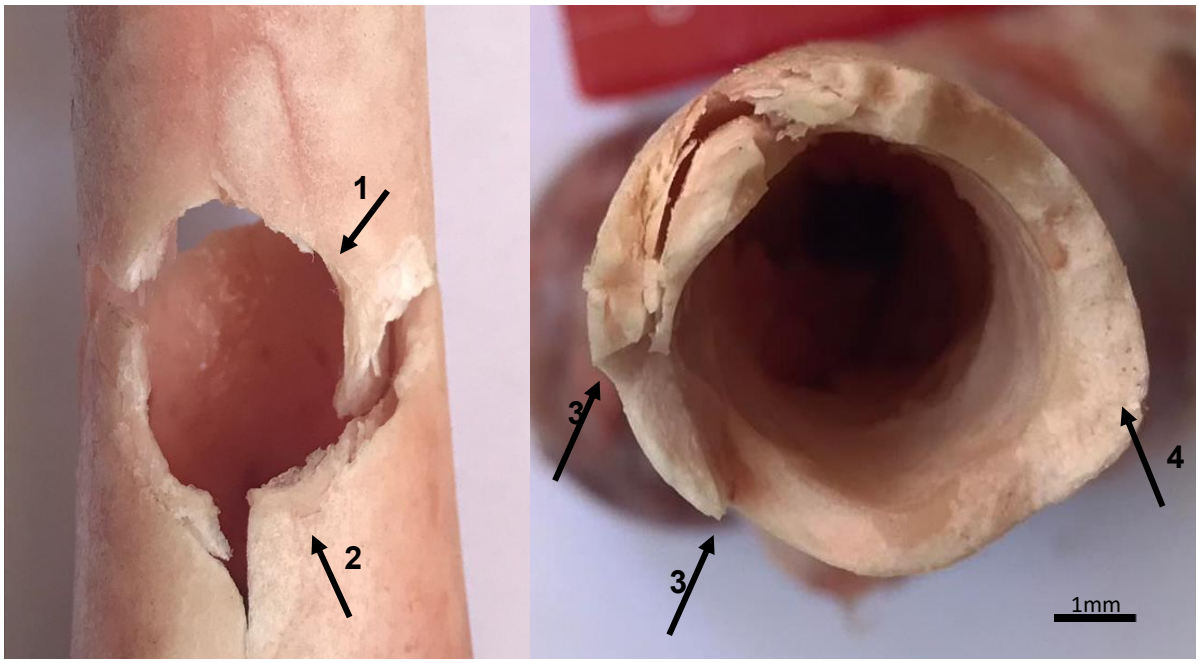

Figure 3.5

Depiction of surface characteristics.

***1)** Crushed margin; **2)** Flaking; **3)** Layered break; **4)** Smooth tension surface.*

Analysis of surface characteristics was performed on the study sample (table 3.7). When applied to the bones which exhibited a complete butterfly fracture, surface morphology had a 100% accuracy. The method was then used to infer directionality of impact for the overall fractured sample and was accurate for 97.1% of the cases.

***Table 3.7**: Accuracy of Inferring Directionality by Assessing Surface Characteristics*

Sample	Accuracy (%)
Complete butterfly fractures (9)	100
Fractured sample (34)	97.1
Total impacted sample (40)	90

4. DISCUSSION

4.1 Skeletal Trauma and Forensic Anthropology

Blunt force trauma patterns may be present in accidental, homicidal and/or abuse cases. It can, therefore, be a strenuous task to accurately reconstruct events leading to death. While the cases share trauma similarities, the patterns in which the fractures are exhibited are different. Forensic anthropologists, consequently, analyse the patterns of trauma and mechanism of injury to accurately reconstruct the events surrounding death (Guyomarc'h *et al.*, 2010; Lefèvre, Alvarez *et al.*, 2015). This also helps in ascertaining the position of the victim and force and velocity of impacts.

The current study aimed to investigate the biomechanics of fractures produced when long bones are subjected to bending as a result of dynamic impacts. An enhanced understanding of the mechanism of injury would allow the refinement of existing methods of trauma pattern analysis and hence, increase the accuracy and reliability of reconstructing the circumstances surrounding the production of fractures.

4.2 Types of Skeletal Trauma

Skeletal trauma varies in its morphological manifestation based on the intensity and magnitude of the extrinsic parameters such as force and energy. This has resulted in the establishment of three main trauma classifications, one of which is blunt force trauma (Davidson *et al.*, 2011; Wedel and Galloway, 2013). .

Within the current study sheep femora were subjected to single dynamic impacts, to the mid-diaphyseal region, to either the anterior or posterior aspect under two energy conditions. Previous studies have demonstrated that impacts to the femur often result in more than one fracture pattern (Kress, 1996; Reber and Simmons, 2015; Cohen *et al.*, 2016; Bertocci *et al.*, 2017). This, therefore, increased the complexity of understanding the biomechanics of fracturing and the subsequent reconstruction of trauma to the lower limbs. Similar findings were noted in the current study with resulting fracture patterns including transverse, linear, butterfly and comminuted or a combination thereof.

However, no oblique fractures were noted during impacts, contrary to studies performed by Cohen *et al.* (2016), Kress (1996), Isa *et al.* (2017) and DeLand (2013), who reported the occurrence of oblique fractures when long bones were subjected to bending. This can be explained through a study performed by Bertocci *et al.* (2017), investigating the fracture patterns between fleshed and defleshed long bones produced during bending which revealed that defleshed bones failed to produce oblique fractures. The lack of oblique fractures during this experiment might also be attributed to the nature of the specimen used. The studies resulting in the production of oblique fractures made use of either porcine or human specimens. This justification is further strengthened by the lack of oblique fractures in the experiment performed by Reber and Simmons (2015). The authors also made use of sheep femora, and their resulting fracture patterns are in agreement with those produced in this current research.

The logistic regression model investigating the influence of side of impact on the production of fractures revealed a weak association. This is supported by a noticeable trend observed with transverse fractures. The majority of transverse lines were produced when bone was impacted on the posterior side. This is in agreement with studies performed by Cohen *et al.* (2017) and DeLand (2013). Cohen *et al.* (2017) noted that the majority of bones subjected to posterior impacts presented transverse lines, while none of the femurs impacted on the anterior side produced transverse fractures. DeLand (2013) found that eight impacted femurs produced transverse fractures, of which five were from bones being impacted posteriorly. While posterior impacts predominantly showed transverse fractures, anterior impacts were largely dominated by the presence of shatter at the point of impact. These results, again, follow the results obtained by Cohen *et al.* (2017), where they found that bones subjected to anterior impacts produced a higher number of fracture lines compared to posterior impacts.

These disparities between anterior and posterior impacts may be explained by the shape of impacting medium and bone geometry. The shaft of the femur cannot be defined as a true cylinder. Sheep femora tend to be flatter on the posterior side along the transverse plane and arch anteriorly with regards to the longitudinal plane. This implies that during anterior impacts, the geometry and curvature of ovine femora naturally oppose the direction of bending during 3-point impacts, contrary to posterior

impacts which mimic the deformation produced during bending impacts (Christensen and Smith, 2013). High speed video footage from Reber and Simmons (2015) showed that anterior impacts resulted in greater deformation as the bending forces opposed the natural curvature of the bone. Furthermore, the anterior surface of the sheep femur is more rounded (Reber and Simmons, 2015). When impacting with a cylindrical t-shaped impactor on the anterior side, a smaller contact area is produced between the surface of the bone and the impactor. This results in the dissipation of energy to a smaller area, thereby generating a high impact stress compared to posterior impacts, where the contact area is broader. An increase in impact stress consequently, results in the production of extensive damage in the form of more fracture lines and/or shattering. (Cohen *et al.*, 2016, 2017).

Of the variables assessed in the current study, none were significantly associated with the production of fractures. There was, however, a weak association between cortical thickness and fracturing of the femora (p=*0.108*). The results depicted by the logistic regressions are in congruence with the results portrayed by Reber and Simmons (2015), who also showed that cortical thickness was of significance. The authors also found that the magnitude of force played a significant role in the production of fractures. The biomechanical principle put forward was that with an increased load, the bone will experience increased strain until failure. The current study investigated the importance of energy instead of force and the results showed that with an increase in impacting energy, sheep bones are twice as likely to fracture. As explained in Section 1.4, energy can be defined as a product of force and therefore, it can be postulated that the same biomechanical principle put forward by Reber and Simmons (2015) applies to the current study in terms of energy. Of the specimens which were subjected to drop tests by these authors, 82% were fractured, which is close to the 85% fracture rate presented in the current study.

4.3 Production of Butterfly Fractures

A butterfly fracture, first defined by Otto Messerer, occurs as a combination of tension, compression and shear forces. When a bone is impacted transversely, tensile forces act on the opposite side of impact, while compression forces act on the side of impact, causing the bone to bend outwards (Thomas and Simmons, 2011; Reber and

Simmons, 2015; Isa *et al.*, 2017). As long bones have evolutionarily adapted to their load-bearing functionality, they tend to be stronger in compression. This results in an initial failure on the side experiencing tension. As the shear strength of the bone is exceeded, the travelling fracture line splits into two, producing a Y-shaped fracture pattern which results in the formation of a triangular breakaway fragment (Gozna *et al.*, 1982; Khor *et al.*, 2006; Passalacqua and Fenton, 2012).

Recently, studies engaging with the biomechanics involved in the production of butterfly fractures have revealed that the theory assuming that the base of the triangular fragment pertains to the side of impact does not always hold true (Reber and Simmons, 2015; Isa *et al.*, 2017). Experimental breaks have shown the occurrence of “false” butterfly fractures, also known as “reverse” butterfly fragments (Rabl *et al.*, 1996; Reber and Simmons, 2015; Scheirs *et al.*, 2017). This suggests that contrary to popular belief, failure may initiate on the side experiencing compression (side of impact), with fracture lines travelling to the side experiencing tension, resulting in the production of a butterfly breakaway fragment, henceforth defined as a compression wedge/lunate (Reber and Simmons, 2015).

While some studies investigating the production of butterfly fractures have only resulted in tension wedges (Martens *et al.*, 1986; Fenton *et al.*, 2012; Khalil *et al.*, 2015), numerous other studies have depicted the occurrence of compression wedges (Kress *et al.*, 1995; Rabl *et al.*, 1996; Thomas and Simmons, 2011; Scheirs *et al.*, 2017). A study led by Kress *et al.* (1995) explored the biomechanics of butterfly fractures using both human femora and tibias. In both cases, compression wedges were produced, 4% and 4.2% respectively. Thomas and Simmons (2011) also showed the presence of compression wedges when sheep femora were impacted. Other studies depicting the presence of compression wedges are Cohen *et al.* (2016), Rabl *et al.* (1996), Reber and Simmons (2015) and Scheirs *et al.* (2017).

Analysis of case studies have also demonstrated the presence of compression fractures. Teresinski and Madro (1999) retrospectively investigated the presence of butterfly fractures in mortuary cases where the victim was hit by a motor vehicle. Of the 34 cases chosen for the study, 12% exhibited compression fractures. The authors reported a total of 41 compression wedges, of which 28 occurred on the tibia and 13 occurred on the femur. Schmidt *et al.* (2016) put forward a case report of a car-

pedestrian traffic accident where autopsy showed the presence of a compression fracture on the femur of the victim. These case studies, along with experimental data, further highlight the incidence of compression wedges and the importance of improving our current understanding behind the biomechanics of butterfly fractures.

During the current experiment, 40% of the fractured bones presented complete butterfly fractures, which is close to the percentage of complete fractures (49%) obtained by Reber and Simmons (2015) when aggregating their specimens impacted by the drop apparatus and pendulum together.

The current sample consisted of four complete wedges and five complete lunates distributed among eight bones.

4.3.1 Butterfly Fractures and Energy

While no significant differences were found for the production of complete butterfly fractures between the two energy groups, post-impact analysis revealed that more butterfly fragments were produced when bones were impacted at a lower energy. Impacts of 22.6 J resulted in the production of six complete butterfly fractures, with three complete tension wedges and three complete lunates. Impacts at 48.56 J resulted in one complete wedge and two complete lunates. These results are dissimilar to those obtained by Cohen *et al.* (2016), where they failed to generate any butterfly fragments at low energy impacts (20.6 J) while their moderate energy impacts (46.7 J) produced a compression wedge. One plausible explanation for this difference would be the high contrast in moment of inertia between the two studies. The regression models run during the current study revealed that moment of inertia was not significant in the production of butterfly fractures. Given that the difference in moment of inertia between the two impact groups was not significant when investigated through a t-test ($p=0.968$), it would imply that the results generated in this study are a true reflection that moment of inertia is not a strong predictor of butterfly fractures. However, the biomechanical principle dictates that an increase in moment of inertia would result in an increase in the fracture resistance of a bone altogether. Consequently, it can be postulated that the reason Cohen *et al.* (2016) failed to produce any butterfly fractures during their low energy impacts is due to their average moment of inertia being 13256mm^4, compared to the current study where the average moment of inertia for the low energy group is 6243.9mm^4. These values imply that the

porcine specimens used by Cohen *et al.* (2016) were more resistant to fracturing in general, compared to the sheep bones used for this study.

Even though more butterfly fragments were produced at low velocity impacts, regression analysis performed showed that energy was of weak significance in the production of butterfly fractures (*p=0.210*). Bone behaves in an elastic manner when impacted at low energy, thereby allowing for bending. At high energy impacts, bone behaves in a more brittle manner and thereby shatters like glass (Currey, 2003a; Porta, 2005). A sensible explanation for the lack of significance of energy revealed in this study might be because the high energy profile in this experiment (48.56 J) still falls within the range of energy reported in the literature (15 J – 118 J) at which butterfly fractures have been produced (DeLand, 2013; Scheirs *et al.*, 2017). Consequently, a much higher energy profile causing bone to behave in a brittle manner (>118 J) might generate different result.

4.3.2 Butterfly Fractures and Cortical Thickness

Contrary to the study performed by Reber and Simmons (2015), the current analysis showed that cortical thickness played a significant role in the production of butterfly fragments. The odds ratio generated (*OR=0.974*) suggests that the production of butterfly fractures is negatively associated with cortical thickness. This implies that an increase in cortical thickness results in decreased chances of producing a complete butterfly fracture. In the current study, due to the random nature of specimen sampling, a difference was noted in the average cortical thickness of the bones in the two energy groups. This difference was tested with a t-test and found to not be significant (*p=0.99*). Thus, the significant role of cortical thickness in butterfly fracture production noted here, is unlikely to be as a result of simple observed differences between the groups. The significance of cortical thickness is strengthened further when analysed with regards to the other variables. The regression models reveal that the results generated for cortical thickness have the highest statistical robustness compared to the others (*p=0.034*).

Cortical thickness is defined as an influencing factor of bone mineral density, which dictates the strength of the bone (Turner, 2002; Hernandez and Keaveny, 2006; Lespessailles and Benhamou, 2007). Furthermore, Norman *et al.* (1995) showed that cortical thickness is directly proportionate to fracture toughness of a bone. From a

biomechanical standpoint, bones exhibiting high bone mineral densities and fracture toughness will have an increased Young's modulus. This implies that the impacted bone will have an enhanced elastic phase and ultimate strain, allowing the bone to better resist bending failure under dynamic loading (Turner, 2002), resulting in an absence of butterfly fracture.

4.3.3 Butterfly Fractures and Side of Impact

Contrary to the results obtained for the production of fractures, null hypothesis regression models showed that impact side influenced the production of complete butterfly fragment. This is reflected in the number of butterfly fractures obtained during this experiment. Of the total fragments produced, seven were obtained when bones were impacted anteriorly, while posterior impacts only resulted in two butterfly fragments. When looking at the totality of butterfly fracture patterns produced, taking into consideration both complete and partial, anterior impacts accounted for 60.9% of the fracture patterns. Posterior impacts accounted for 39.1%.

These results are in agreement with previous studies investigating the importance of loading direction in the production of butterfly fractures. Reber and Simmons (2015) also reported an increased production of butterfly fragments from anterior impacts compared to posterior impacts. While the authors do not report the number of butterfly fractures produced during anterior and posterior impacts respectively, their statistical analyses suggested that anterior impacts were 69.7 times more likely to produce butterfly fragments while posterior impacts were 151.9 times more likely to produce a non-butterfly fracture. It was suggested that the discrepancy of fracture patterns between anterior and posterior impacts may be due to an overall fracture resistance difference between the two sides. This can be better explained through the transfer and diffusion of energy from the impactor to the impacted surface. As mentioned previously, the anterior surface of the femur is more rounded than the posterior surface. When impacted, the contact point is consequently, smaller on the anterior surface, resulting in an increased localised pressure compared to posterior impacts, causing the bone to bend more acutely (Cohen *et al.*, 2016, 2017). Additionally, the increased energy diffusion on the anterior aspect results in failure on the compression side. This statement is supported by the high number of shattered impact points observed during anterior impacts performed in this experiment.

4.4 Inferring Directionality from Butterfly Fractures

During forensic reconstructions, anthropologists make use of butterfly fractures to infer directionality of impact. The current theory, referred to as Messerer's theory, dictates that side of impact relates to the base of the wedge (compression) while the apex is a product of initial failure due to tension. However, recent studies have depicted that this theory is flawed in two major ways. Firstly, the Messerer theory does not account for the occurrence of compression fractures and assumes that all butterfly fractures are tension wedges. Additionally, the theory is only applicable to cases where impact has led to the production of a detached butterfly fragment (Teresinski and Madro, 1999; Reber and Simmons, 2015; Schmidt *et al.*, 2016; Isa *et al.*, 2017).

Teresinski and Madro (1999) extended this theory to their case studies and revealed that it could be applied to only 54% of their sample. This implies that in their case, the use of Messer's theory to infer directionality from butterfly fragments had a 46% inaccuracy.

Reber and Simmons (2015) also applied the theory to their experimental sample and found that it was only 60% accurate when applied to specimens that produced a butterfly fragment. One suggestion made by these authors was to account for fragment angle. The authors proposed that butterfly fragments formed in compression had an obtuse apex, compared to a tension wedge with an acute apex, which improved accuracy of inferring directionality from butterfly fractures to 97%. However, a major issue which remains is that this principle, similar to the Messerer theory, requires the production of a detached butterfly fragment during impact. The authors did report that both theories were only applicable to 44% of their total sample. When looking at their overall fractured sample, the Messerer technique and the fragment angle theory has accuracies of 29% and 47% respectively.

Another method of inferring directionality proposed by Reber and Simmons (2015) consisted of accounting for partial tension and compression fracture patterns. This principle was applicable to 83.9% of the overall fractured sample and had an accuracy of 82.6%.

In the current study, 40 sheep femora were impacted, of which 34 were fractured. A total of 9 complete butterfly fragments were obtained, and 14 partial fractures. Three methods of inferring directionality were applied to investigate their levels of accuracy.

Directionality was first inferred using the Messerer method. Given that it requires the presence of a detached butterfly fragment, it was only applicable to 26.5% of the overall fractured sample. The issue of assuming that all butterfly fractures are tension wedges was further highlighted during the analysis. When applied to the detached butterfly sample, the accuracy of the Messerer technique was only of 22%. When applied to the overall fractured sample, the accuracy of the method decreased to 5.9%.

The second principle used was the fragment angle method proposed by Reber and Simmons (2015). Again, it was only applicable to 26.5% of the fractured sample due to its restrictive requirement of a detached piece. Of the nine butterfly fragments obtained during this experiment, the method was only able to accurately infer side of impact for six fragments, resulting in an accuracy of 66.7%. Three of the produced compression wedges exhibited acute angle fragments and were consequently classified as tension wedges, resulting in the erroneous deduction of side of impact. The overall accuracy of the method when including all the fractured femora was only 17.6%.

Lastly, directionality was inferred by using a combination of fragment angle and partial butterfly fracture patterns. This method was applicable to 67.6% of the fractured sample. In this scenario, the percentage accuracy was increased to 87% when applied to bones exhibiting butterfly fracture patterns. The overall accuracy of the method when applied to all fractured bones was 59%.

From the three methods employed to infer directionality from the fractured bones, the principle of using fragment angle alongside partial butterfly fracture patterns was revealed to be the most accurate one. Nonetheless, the method was still restrictive as it could only be applied to bones exhibiting either complete and/or partial butterfly patterns. Directionality of impact could not be determined for bones which did not produce any butterfly patterns.

4.4.1 Understanding the Importance of Fracture Surface Morphology

Given the levels of accuracy of the existing methods of inferring directionality of impact, there is a high need for a more reliable and accurate method. Biomechanical studies investigating fractures in bones have ascertained that tension and compression surfaces can be differentiated through their respective morphological characteristics. Tension surfaces usually have a smooth and billowy appearance, suggestive of tearing. Compression surfaces, on the other hand, have an extensive range of characteristics (Symes *et al.*, 2012; Iscan and Steyn, 2013; Isa *et al.*, 2017; Scheirs *et al.*, 2017). The most common feature that arises when bone fails in compression is layered breakage, which occurs on the cortical bone. A layered break is often accompanied by a crushed margin which occurs on the edge of the fracture and has a scale-like appearance. Lastly, compression breaks may result in the production of a bone flake, which can be described as superficial peeling of the cortical bone (Scheirs *et al.*, 2017).

In the current study, directionality was also inferred using a combination of surface characteristics and overall butterfly fracture pattern morphology. The percentage accuracy of determining direction of side of impact for the samples that resulted in butterfly fracture patterns was 100%. This method was then applied to the overall fractured sample and directionality was inferred correctly for all but one specimen, resulting in an accuracy of 97.1%. The specimen to which the method could not be applied was fractured as a result of pure tension, thereby all the surfaces exhibited tension characteristics. The advantage of using overall fracture morphology in combination with surface features is that the method does not require the presence of a detached piece. Furthermore, it could be applied to samples which did not exhibit butterfly fracture patterns, and even to some extent to bones which failed to fracture. From the six bones which failed to fracture, impact point could be determined for three of them by assessing surface morphology. The other three failed to show any surface characteristics visible to the naked eye. Consequently, when applied to the overall sample impacted, the percentage accuracy of determining directionality was 90%. None of the three existing methods tested during the study could be applied to the overall impacted sample.

4.5 Limitations and Further Improvements

Although the principles put forward in this study may be applied to human bones, the results obtained are sample specific. Additionally, the study was restricted in terms of sample size. Further validation with a bigger sample size is advised to improve and ascertain the robustness of the results generated in this study. Furthermore, a bigger sample size would allow for further investigation of fracture production at higher energies, allowing for better investigation of the significance of energy in the production of butterfly fractures. Additionally, lateral and medial loading directions would also be assessed through a bigger sample size.

Axial loading and its effect on the production of butterfly fractures were not investigated in the current study. Limited studies have been conducted to directly investigate whether the presence or absence of axial loading significantly alters the production of butterfly fractures. While some studies have shown that butterfly fractures can be produced without the presence of axial loading (Thomas and Simmons, 2011; Khalil, 2015; Scheirs *et al.*, 2017), others have demonstrated that axial loading influences the fracture patterns produced during three point bending impacts (Cohen *et al.*, 2016, 2017). The study performed by Cohen et al. (2017) also revealed that the presence of axial loading generates bigger butterfly fragments. Future research investigating the importance of axial loading during dynamic bending impacts is therefore, encouraged as its application to bone during impact may yield different results and/or be closer to impacts happening in real-life scenarios. This will aid in refining the current methods of trauma pattern analysis along with prevailing knowledge about fracture biomechanics in long bones.

The bones used for this study were defleshed to allow for proper orientation during impact and ascertain complete transfer of energy from the impactor to the bone, which was necessary for the purpose of this study. Furthermore, this allowed for better comparison with previous studies which also removed the flesh prior to impact. Additionally, the principle of energy diffusion through soft tissue is still unexplored in the forensic literature (DeLand, 2013; Reber and Simmons, 2015; Isa *et al.*, 2017). Further studies on soft tissue resistance is needed to obtain a more accurate understanding of the biomechanics involved in the production of butterfly fragments

during blunt force trauma. These will help in more accurate reconstructions about velocity, force and energy of impact.

The impactor used in this study was a hollow tube. A major issue was the rotation and stabilisation of the impactor during the drop test. Consequently, transverse impact could not be standardised across all bones as rotation resulted in the impactor hitting the femur parallel to the longitudinal axis for some specimens. The use of a spherical impactor would be better suited for such research as this would increase the consistency of contact point area during impacts. Furthermore, this would also standardise the amount of energy transferred during impact as the contact area would be uniform for all the impacted femora.

As mentioned in Section 4.5, some non-fractured specimens could not be analysed as the surface characteristics of the impact point were not visible to the naked eye. The use of a stereo microscope for the analysis of surface morphology might reveal further characteristics which can be used for better differentiation between tension and compression surfaces. While the investigation of micro characteristics was beyond the scope of this study, additional studies investigating the micro surface morphology through scanning electron microscopy of the impacted surface might also help better understand the propagation and angle shift of the fracture lines resulting in butterfly pattern formation.

5. CONCLUSION

When faced with skeletonised remains, the medicolegal system often requires the assistance of forensic anthropologists to reconstruct the identity of the victim and determine cause and events leading to death. While the framework dealing with the analysis of skeletal blunt force trauma is well established in the forensic field, the biomechanical aspect of some fractures still has a degree of uncertainty. One such area is the inference of impact direction in dynamic loading events. Currently, forensic anthropologists apply the traditional theory developed by Messer (1880) using butterfly fragments.

More recent studies have shown that this principle is flawed as it assumes that all butterfly fragments are tension wedges. The occurrence of 'false' butterfly fractures, now referred to as compression wedges, has been proven through both experimental impacts and retrospective analysis of case studies involving blunt force trauma to the lower limb. Furthermore, the current theory restricts the analysis of wedge fractures as it demands the presence of a detached piece. There is, consequently, a need to better understand the biomechanics involved in the production of butterfly fractures in order to devise a more reliable method of analysis.

This current study has further confirmed the presence of compression wedges during impacts to long bones. Of the complete butterfly fragments produced, 55.6% were compression wedges. From a biomechanical standpoint, the results suggest that a new theory about the formation of butterfly fractures is required.

The results showed that none of the variables tested were significant for the fracturing of bones except for cortical thickness, which shared a relatively weak association with the production of fractures. Cortical thickness was also found to contribute to the production of complete butterfly fractures. In both scenarios, odds ratios revealed that the variable negatively correlated to fracturing and butterfly fracture formation. Additionally, the regression models showed that geometry of side of impact was highly significant during bending impacts resulting in wedge fractures and that anterior impacts were 5.14 times more likely to produce complete butterfly fractures compared to posterior impacts. This was supported by the difference in the number of butterfly fractures presented during anterior (78%) and posterior impacts (22%).

One of the objectives of the study was to investigate the reliability and accuracy of the existing methods of inferring directionality from the analysis of butterfly fractures. The results obtained have demonstrated that the prevailing principles can be restrictive as they either require the presence of detached pieces or work on assumptions that are not always true. While the theory established by Messerer was proven to be accurate to only 5.9%, the alternative methods of angle fragment and fracture morphology put forwards by Reber and Simmons were only 17.6% and 59% accurate, respectively. Such levels of accuracy are still too low to be of evidentiary value. The current study has established that the incorporation of fracture surface features along with the analysis of overall fracture pattern morphology provides a more reliable method of analysis. When applied to the current sample, the percentage of inferring directionality from complete butterfly fractures was increased to 100% and 97.1% to the overall fractured sample. Contrary to the existing method, this theory does not require the presence of a butterfly fracture and consequently, has the potential to be applied to bones that exhibit other fracture patterns. It can, therefore, be useful in minimising the current margin of error which prevails in the analysis and reconstruction of butterfly fractures as well as injuries to long bones in general. The method explored in this study can thus better assist forensic anthropologists in their analyses of medicolegal cases involving blunt force trauma.

6. REFERENCES

1. Alms, M. (1961) 'Fracture mechanics', *Journal of Bone and Joint Surgery,* 43(1):162-166.

2. Ambade, V. N. and Godbole, H. V. (2006) 'Comparison of wound patterns in homicide by sharp and blunt force', *Forensic Science International,* 156(2-3):166-170.

3. Bertocci, G., Thompson, A. and Pierce, M, C. (2017) 'Femur fracture biomechanics and morphology associated with torsional and bending loading conditions in an in vitro immature porcine model', *Journal of Forensic and Legal Medicine,* 52:5-11.

4. Clark, C., Mole, C. G. and Heyns, M. (2017) 'Patterns of blunt force homicide in the West Metropole of the City of Cape Town, South Africa', *South African Journal of Science,* 113(5):1-6.

5. Cohen, H., Kugel, C., May, H., Medlej, B., Stein, D., Slon, V., Hershkovitz, I. and Brosh, T. (2016) 'The impact velocity and bone fracture pattern: Forensic perspective', *Forensic Science International,* 266:54-62.

6. Cohen, H., Kugel, C., May, H., Medlej, B., Slon, V, Brosh, T. and Hershkovitz, I. (2017) 'The influence of impact direction and axial loading on the bone fracture pattern', *Forensic Science International,* 277:197-206.

7. Cooke, F. W., Zeidman, H. and Scheifele, S. J. (1973) 'The fracture mechanics of bone- Another look at composite modelling', *Journal of Biomedical Materials Research,* 7(3):383-399.

8. Christensen A, Smith V. (2013) 'Rib butterfly fractures as a possible indicator of blast trauma', *Journal of Forensic Sciences,*58(SI):S15–9.

9. Currey, J. D. (2003a) 'How well are bones designed to resist fracture?', *Journal of Bone and Mineral Research,* 18(4):591-598.

10. Currey, J. D. (2003b) 'Role of collagen and other organics in the mechanical properties of bone', *Osteoporosis International,* Suppl. 5 (September, 14): S29-36.

11. Davidson, K., Davies, C. and Randolph-Quinney, P. (2011) 'Skeletal Trauma', in *Forensic Anthropology: 2000-2010.* Black, S. and Ferguson, E, Eds. Florida: CRC Press. 183-235.

12. Delahay, J. N. and Sauer, S. (2007) 'Skeletal Trauma', in *Essentials of Orthopedic Surgery*. Wiesel, S. W. and Delahay, J. N, Eds. 3rd ed. New York: Springer-Verlag. 40-83.

13. DeLand, T. (2013) *Studies on the development and fracture mechanics of cortical bone.* M.Sc Thesis. Michigan State University.

14.Dempsey, N., Gilbert, F. M., Miszkiewicz, J. and Oxenham, M. (2018) 'Biomechanical analysis of controlled tibial blunt force trauma', *Australian Journal of Forensic Science*. (in press) DOI: 10.1080/00450618.2018.1429017

15. Fenton, T. W., Kendell. A, E., DeLand, T, S. and Haut, R. C. (2012) 'Determination of impact direction based on fracture patterns in human long bones', in *Proceedings of the 64th Annual Scientific Meeting of the American Academy of Forensic Sciences,* 25-25 February 2012. Atlanta, GA.

16. Galloway, A. and Zephro, L. (2005) 'Skeletal trauma analysis of the lower extremity', in *Forensic Medicine of the Lower Extremity: Human Identification and Trauma Analysis of the Thigh, Leg and Foot.* Rich, J., Dean, D. and Powers, R, Eds. New Jersey: Humana Press. 253-277.

17. Gozna, E., Harrington, I. and Evans, D. (1982) *Biomechanics of Musculoskeletal Injury.* Baltimore: Williams & Wilkins.

18. Guyomarc'h, P., Campagna-Vaillancourt, M., Kremer, C. and Sauvageau, A. 'Discrimination of falls and blows in blunt head trauma: a multi-criteria approach', *Journal of Forensic Sciences,* 55(2):423-427.

19. Hernandez, C. J. and Keaveny, T. M. (2006) 'A biomechanical perspective on bone quality', *Bone*, 39(6):1173-1181.

20. Hipp, J. A. and Hayes, W. C. (2013) ‘Biomechanics of fractures’, in *Skeletal Trauma: Basic Science, Management and Reconstruction.* Browner, B. D., Levine, A. M., Jupiter, J. B. and Trafton, P. G, Eds. 3rd ed. Pennsylvania: Elsevier Science. 90-119.

21. Isa, M. I., Fenton, T. W., DeLand, T. and Haut, R. C. (2017) ‘Assessing impact direction in 3-pont bending of human femora: Incomplete butterfly fractures and fracture surfaces’, *Journal of Forensic Sciences,* 63(1):38-46.

22. Iscan, M. Y. and Steyn, M. (2013) *The Human Skeleton in Forensic Medicine.* 3rd ed. Illinois: Charles C Thomas Publisher LTD.

23. Katz, E. P. and Li, H. (1973) ‘Structure and function of bone collagen fibrils’, *Journal of Molecular Biology,* 80:1-15.

24. Khalil, A., Raymond, D., Miller E. A. (2015) ‘An analysis of butterfly fracture propagation’ in *Proceedings of the 67th Annual Scientific Meeting of the American Academy of Forensic Sciences,* 16-21 February 2015. Orlando, FL.

25. Khor, F., Watson, B., Gierczycka, D., Malcolm, S., Panzer, M. B. and Cronin, D. (2016) ‘Effects of cortical bone material asymmetry using a three-point bend test simulation’, in *Proceedings of 2016 International Research Council on Biomechanics of Injury Conference,* 16-18 May 2016. Seoul, Korea.

26. Kieser, J., Taylor, M. and Carr, D. (2013) *Forensic Biomechanics.* Sussex: John Wiley & Sons, Ltd.

27. Kimmerle, E. H. and Baraybar, J. P. (2008) *Skeletal Trauma: Identification of Injuries Resulting from Huan Rights Abuse and Armed Conflict.* Illustration Ed. Boca Raton: CRC Press.

28. Kress, T. A., Porta, D. J., Snider, J. N., Fuller, M. P., Psihogios, J. P., Heck, W. L., Frick, S. J. and Wasserman, J. F. (1995) ‘Fracture patterns of human cadaver long bones, in *Proceedings of 1995 International Research Council on Biomechanics of Injury Conference,* 13-15 September 1995. Brunnen, Switzerland.

29. Kress, T. A. (1996) *Impact Biomechanics of the Human Body.* Ph.D. Thesis. University of Tennessee.

30. Lanyon, L. E., Goodship, A. E., Pye. C. J. and MacFie, J. H. (1982) 'Mechanically adaptive bone remodelling', *Journal of Biomechanics,* 15(3):141-154.

31. Lefèvre, T., Alvarez, J. C. and Lorinf de Grandmaison, G. (2015) 'Discriminating factors in fatal blunt trauma from low level falls and homicide', *Forensic Science Medicine and Pathology,* 11(2):152-161.

32. Lerer, L. B., Matzopoulous, R. G. and Phillips, R. (1997) 'Violence and injury mortality in the Cape Town Metropole', *South African Medical Journal,* 87(3):298-301.

33. Lespessailles, E. and Benhamou, C. (2007) 'Evaluation of macrostructural bone biomechanics', *Joint Bone Spine*, 74(3):233-239.

34. Lovell, N. C. (1997) 'Trauma analysis in paleopathology', *Yearbook of Physical Anthropology,* 170(40):193-170.

35. Martens, M., van Audekercke, R., de Meester, P. and Mulier, J. C. (1986) 'Mechanical behaviour of femoral bones in bending loading', *Journal of Biomechanics,* 19(6):443-454.

36. Martin, B. R., Burr, D. B. and Sharkey, N. A. (1998) *Skeletal Tissue Mechanics,* New York: Springer-Verlag.

37. Matzopoulous, R., Prinsloo, M., Pillay-van Wyk, V., Gwebushe, N., Mathews, S., Martin, L. J., Laubscher, R., Abrahams, N., Msemburi, W., Lombard, C. Bradshaw, D. (2015) 'Injury-related mortality in South Africa: a retrospective descriptive study of postmortem investigations', *Bulletin of the World Health Organization,* 93(5):303-313.

38. Messerer, O. (1880) *Über Elasticität und Festigkeit der menschlichen Knochen,* Cotta, Stuggart.

39. Mole, C., Heyns, M. and Cloete, T. (2015) ‘How hard is hard enough ? An investigation of the force associated with lateral blunt force trauma to the porcine cranium’, *Legal Medicine*. 17(1):1–8.

40. Mubeen, B., Ahmed, I. and Jameel, A. (2015) ‘Study of the mechanical properties of bones and mechanics of bone fracture’, in *Proceedings of the 60th Congress of the Indian Society of Theoretical and Applied Mechanics*. 16-19 December 2015. Jaipur, Rajasthan.

41. Norman, T. L., Vashishth, D. and Burr, D. B. (1995) ‘Fracture toughness of human bone under tension’, *Journal of Biomechanics,* 28(3):309-320.

42. Oyen, M. L. and Ferguson, V. L. (2010) ‘Bone as a Composite Material’, in *Biomechanics of Hard Tissues: Modeling, Testing, and Materials*. Öchsner, A. and Ahmed, W, Eds. Weinheim: Wiley. 101–122.

43. Passalacqua, N. V and Fenton, T. W. (2012) ‘Developments in Skeletal Trauma: Blunt-Force Trauma’, in *A Companion to Forensic Anthropology*. Dirkmaat, D. C, Ed. Oxford:Wiley-Blackwell. 400–412.

44. Porta, D. J. (2005) ‘Biomechanics of Impact Injury’, in *Forensic Medicine of the Lower Extremity: Human Identification and Trauma Analysis of the Thigh, Leg and Foot*. Rich, J., Dean, D., and Powers, R, Eds. New Jersey: Humana Press. 279–310.

45. Rabl, W., Haid, C. and Krismer, M. (1996) ‘Biomechanical properties of the human tibia: fracture behavior and morphology.’, *Forensic Science International*, 83(1):39–49.

46. Rastogi, S., Duthie, B. and Wild, B. R. (1986) ‘Biomechanical aspects of femoral fractures in automobile’, *Journal of Bone and Joint Surgery*, 68-B(5):760–766.

47. Ravi-Chandar, K. and Knauss, W. G. (1984) ‘An experimental investigation into dynamic fracture : II . Microstructural aspects’, *International Journal of Fracture*, 26(1):65–80.

48. Reber, S. L. and Simmons, T. (2015) ‘Interpreting Injury Mechanisms of Blunt Force Trauma from Butterfly Fracture Formation’, *Journal of Forensic Sciences*, 60(6):1401–1411.

49. Reznikov, N., Shahar, R. and Weiner, S. (2014) ‘Bone hierarchical structure in three dimensions’, *Acta Biomaterialia*,10(9):3815–3826.

50. Rho, J., Kuhn-Spearing, L. and Zioupos, P. (1998) ‘Mechanical properties and the hierarchical structure of bone’, *Medical Engineering & Physics*, 20(2):92–102.

51. Ruff, C., Holt, B. and Trinkaus, E. (2006) ‘Perspectives Who ’ s Afraid of the Big Bad Wolff ? : “‘ Wolff ’ s Law ”’ and Bone Functional Adaptation’, *American Journal of Physical Anthropology*, 129:484–498.

52. Safadi, F. F., Barbe, M., Abdelmagid, S., Rico, M., Aswad, R. A., Litvin, J. and Popoff, S. N. (2009) ‘Bone structure, develoment and bone biology’ in *Bone Pathology.* Khurana, J, S, Ed. Philadelphia: Humana Press. 1-50.

53. Scheirs, C., Malgosa, A., Sanchez-Molina, D., Ortega-Sanchez, M., Velaquez-Ameijide, J., Arregui-Dalmases, C., Medallo-Muniz, J. and Galtes, I. (2017) ‘New insights in the analysis of blunt force trauma in human bones . Preliminary results’, *International Journal of Legal Medicine,* 131(3):867-875.

54. Schmidt, S. C., Schulz, R. R., Pfeiffer, H. M., Schmeling, A. and Geserick, G. (2016) ‘On the evidential value of a Messerer fracture sustained in car- pedestrian traffic accident’, *International Journal of Legal Medicine*, 130(6):1593–1597.

55. Sharir, A., Barak, M. M. and Shahar, R. (2008) ‘Whole bone mechanics and mechanical testing’, *The Veterinary Journal*, 177(1): 8–17.

56. Sharkey, E. J., Cassidy, M., Brady, J., Gilchrist, M. D. and NicDaeid, N. (2011) ‘Investigation of the force associated with the formation of lacerations and skull fractures’, *International Journal of Legal Medicine*, 126(6):835–844.

57. Symes, S., L’Abbé, N. E., Chapman, E. N., Wolff, I. and Dirkmaat, D. C. (2012) ‘Interpreting traumatic injury to bone in medicolegal investigation’, in *A Companion to Forensic Anthropology*. Dirkmaat, D. C, Ed. Oxford: Blackwell Publishing. 340–389.

58. Teresinski, G. and Madro, R. (1999) ‘The Evidential Value of Wedge-Shaped Tibial and Femoral Fractures in Cases of Car-to- Pedestrian Collisions’, *Problems of Forensic Science,* 40(XL):72–85.

59. Tersigni-Tarrant, M. A. and Shirley, N. R. (2013) *Forensic Anthropology: An Introduction*. Oxford:CRC Press.

60. Thieme, S. and Wingren, M. (2009) *Understanding fracture mechanisms of the upper extremities in car accidents*. B.Sc Thesis. Halmstad University.

61. Thomas, T. S. and Simmons, T. (2011) 'The Relationship Between Directionality of Force and the Formation of Butterfly Fractures', in *Proceedings of the 63rd Annual Scientific Metting of the American Academy of Forensic Sciences*. Chicago. 21-26 February 2011. Chicago, IL.

62. Torimitsu, S., Nishida, Y., Takano, T., Koizumi, Y., Hayakawa, M., Yajima, D., Inokuchi, G., Makino, Y., Motonura, A., Chiba, F. and Iwase, H. (2014) 'Effects of the freezing and thawing process on biomechanical properties of the human skull', *Legal Medicine*, 16(2):102-105.

63. Turner, C. H. (2002) 'Determinants of Skeletal Fragility and Bone Quality', *Osteoporosis International*, 13(2):97–104

64. Wedel, V. and Galloway, A. (2013) *Broken Bones: Anthropological Analysis of Blunt Force Trauma*. 2nd Ed. Illinois: Charles C Thomas. Publisher LTD.

65. Wolff, J. (1982) *The Law of Bone Remodelling*. Berlin: Springer-Verlag.

66. Wright, T. M. and Hayes, W. C. (1976) 'The Fracture Mechanics of Fatigue Crack Propagation in Compact Bone', 648(7), pp. 637–648.

67. Young, H. D., Freedman, R. A. and Ford, L. A. (2008) *Sears and Zemansky's University Physics*. 12th Ed. New York: Pearson.

68. Yukawa, N., Kojimahara, M., Green, M. A., Saito, T., Osawa, M and Takeichi, S. (1997) 'A Messerer fracture', *Forensic Science International*, 88(3):231–234.

APPENDIX A: ETHICS APPROVAL LETTER

UNIVERSITY OF CAPE TOWN
Faculty of Health Sciences
Animal Ethics Committee

Room E52-24 Old Main Building
Groote Schuur Hospital
Observatory 7925
Telephone [021] 406 6492
Email: sumayah.arefdien@uct.ac.za
Website: www.health.uct.ac.za/fhs/research/animalethics/forms

10 December 2018

Dr C Mole
Division of Forensic Medicine &
Toxicology
Entrance 3 Level 1
Falmouth Building-FHS

Dear Dr Mole

PROTOCOL TITLE: Understanding the mechanism of injury associated with long bone fractures through dynamic bending impact

FHS AEC REF NO: 018/044

Thank you for submitting your request for approval of use of animal material for scientific purposes to the Faculty of Health Sciences (FHS) Animal Ethics Committee (AEC).

I am pleased to inform you that the FHS AEC EXCO has **approved** your request, which will terminate on **30 December 2021.**

Number of animal material & species: Ovis Aries (sheep) 60 specimens
Please quote the FHS AEC REF NO (above) in all future correspondence.

Please note that the approval of this protocol imposes the following obligations on the principal investigator (PI):

1. To submit an annual mandatory progress report. The first annual report for this protocol is due on **28 February 2019.** The forms can be accessed from http://www.health.uct.ac.za/fhs/research/animalethics/forms
2. To submit a final mandatory report on the **30 December 2021,** please access the final report form from: http://www.health.uct.ac.za/fhs/research/animalethics/forms

3. Ensuring that all study participants perform within the confines of the procedures and experimental design of the protocol as approved, or as amended.
4. Ensuring that all study participants comply with all applicable national legislation, UCT policies, FHS AEC policies and standard operating procedures (SOPs) and national standards (SANS 10386: 2008).

My best wishes for a successful research and /or teaching endeavour.

Yours sincerely

pp.

PROF PJ COMMERFORD
CHAIR, FHS AEC

AEC REF# 018/044

APPENDIX B: RAW DATA

Specimen #	Impact Site	Bone Length\ /mm	External Antero-posterior diameter/ mm	Internal Antero-posterior diameter/ mm	External Medio-lateral diameter/ mm	Internal Medio-lateral diameter/ mm	Anterior Thickness/ mm	Posterior Thickness/ mm	Lateral Thickness/ mm	Medial Thickness/ mm	Moment of Inertia/ mm^4	Fractured	Morphology/Type	Overall Extent of Fracture /mm	Description
DROP HEIGHT: 1m; WEIGHT: 2.3 kg; ENERGY: 22.6 J															
UCT/18/ 01	Anterior	174	18.1	13.34	18.04	12.16	3.26	2.56	3.18	3.02	**3**713.95 7285	Yes	1. Complete wedge and complete lunate 2. Partial Wedge	31.88	1. The detached piece shows both lunate (posterolateral) and wedge (postermedial) morphlogy 2. Partial wedge present on the medial side
UCT/18/ 02	Anterior	211	23.8	16.18	22.76	16.18	3.1	3.38	2.68	3.34	12385.6 8058272 98	Yes	1. Complete lunate 2. Longitudinal fracture lines on anterior surface	112.76	1. Extensive shattering on impact point 2. Compression surfaces show extreme flaking 3. Tension surfaces are smooth with minimal bollowing; detached piece only has tension surfaces
UCT/18/ 03	Anterior	176	17.76	15.28	17.26	15.14	3.14	3.32	2.86	3.08	2207.75 9103	Yes	1. Lunate pieces on both lateral and medial side	70.82	1. Extensive shattering on impact point with missing pieces 2. Compression surfaces are jagged and concentrated at impact point 3. All detached pieces show tension surfaces with evidence of tearing
UCT/18/ 04	Anterior	178	18.94		18.24							No	DISCARDED AS IMPACT WAS TOO CLOSE TO EPIPHYSIS		

UCT/18/05	Anterior	216	27.06	19.22	24.02	19.42	3.2	2.96	3.42	3.68	19621.11752	Yes	1. Comminuted (> 3 pieces)	131.26	1. Extreme shattering 2. Linear fracture lines radiating from point of impact 3. All fractured surfaces show tension characteristics apart from impact point
UCT/18/06	Anterior	202	24.52	20.6	24.12	20.02	3.24	3.12	3.04	3.24	8904.284009	No	1. Concentric and linear fracture lines	69.78	1. Concentric fracture lines depicting point of impact 2. Inwards bevelling with extreme flaking on impact point 3. Linear fracture line on anterior surface radiating from impact point
UCT/18/07	Anterior	196	21.98	17.6	20.78	15.52	3.4	3.84	2.92	3.48	6747.260554	Yes	1. Partial lunate 2. Comminuted	119.16	1. Small compressive surface depicting point of impact 2. All fractured surfaces show evidence of tearing in tension 3. Partial lunate on medial side
UCT/18/08	Anterior	199	20.02	13.04	19.92	15.42	2.86	3.42	2.98	2.82	6466.124906	Yes	1. Comminution	N/A	1. Intensive shattering at impact point 2. Flakes showing compression 3. All fractures on anterior surface
UCT/18/09	Anterior	201	19.24	13.46	19.82	14.42	3.04	4.52	2.96	3.28	5115.313303	Yes	1. Comminution 2. Partial lunate	N/A	
UCT/18/10	Anterior	190	21.78	14.86	19.92	14.32	4.36	4.32	3.48	2.86	8652.34295	No	N/A	N/A	N/A
UCT/18/11	Anterior	188	20.08	13.54	19.86	14.74	4.34	5.22	3.62	3.16	6330.550974	No	N/A	N/A	N/A
UCT/18/12	Posterior	183	20.22	14.42	18.44	12.26	3.44	2.36	2.48	2.82	6082.882648	Yes	1. Comminution	67.56	1. Clearly defined compression features at point of impact
UCT/18/13	Posterior	164	17.76	13.14	17.12	11.58	3.1	3.44	2.76		3420.258054	Yes	1. Transverse fracture 2. Partial Wedge	31.52	1. Partial wedge on anterior surface 2. Compressive surfaces not visible

UCT/18/ 14	Posterior	165	18.36	12.66	17.06	11.08	4.14	2.88	3.14	2.72	4316.80 0148	Yes	1. Transverse fracture 2. Longitudinal fracture 3. Partial lunate	60.36	1. Partial lunate on anterolateral surface 2. Compressive surfaces not visible
UCT/18/ 15	Posterior	168	18.1	11.08	17.86	11.54	4.42	3.24	3.48	3.18	4528.64 1307	Yes	1. Transverse fracture 2. Bone chip	20.62	1. Clearly defined compression features at point of impact 2. Bone chip on anterior surface
UCT/18/ 16	Posterior	164	16.98	14.08	16.94	10.96	3.52	2.96	3.02	2.88	2151.35 3712	Yes	1. Transverse fracture 2. Complete wedge	28.56	1. Wedge fracture on medial surface 2. Compression surfaces clearly defined
UCT/18/ 17	Posterior	175	18.06	10.78	17.6	10.6	4.54	3.58	3.82	3.92	4559.15 2975	Yes	1. Transverse fracture 2. Partial wedge	18.68	1. Partial wedge on medial surface 2. Compression surfaces clearly defined
UCT/18/ 18	Posterior	175	17.84	10.32	18.36	11.38	3.7	3.78	3.36	3.16	4415.42 1636	Yes	1. Transverse fracture 2. Bone chip	15.84	1. Bone chip medial surface 2. Compression surfaces clearly defined
UCT/18/ 19	Posterior	193	18.44	11.36	18.18	10.84	3.72	3.62	3.42	4.26	4858.13 1875	Yes	1. Transverse fracture 2. Bone chip 3. Partial lunate	31.84	1. Partial lunate on posterolateral side 2. Bone chips on both lateral and medial sides
UCT/18/ 20	Posterior	190	19.12	12.68	18.44	12.76	3.44	4.52	3.14	2.76	5291.30 9	No	1. Depression at site of impact with minimal flaking	13.02	1. Presence of flakes/scales
UCT/18/ 21	Posterior	191	18.74	11.78	18.14	11.12	4.26	3.24	3.64	3.58	5108.82 1725	Yes	1. Transverse fracture 2. Complete lunate	44.96	1. Clearly defined compression surfaces 2. Lunate on posterior side
DROP HEIGHT: 1.5m ; WEIGHT: 3.3 kg ; ENERGY: 48.56 J															
UCT/ 18/ 24	Anterior	192	18.36	14.02	18.44	12.86	3.46	3.54	2.48	3.04	3681.23 0286	Yes	1. Comminution 2. Complete lunate	64.12	1. Extreme shattering at point of impact 2. Incomplete linear lines along shaft 3. Complete lunate on anterior side
UCT/ 18/ 25	Anterior	199	21.58	13.92	19.72	13.24	3.84	4.36	3.44	3.18	8802.72 8832	Yes	1. Comminution 2. Complete lunate	60.56	1. Extreme shatter 2. Lunate on anterior side

UCT/ 18/ 26	Anterior	196	20.54	14.6	19.82	13.66	4.04	4.18	3.08	3.32	6506.79 4867	Yes	1. Partial wedge	119.44	1. Point of impact missing due to shatter 2. Linear fracture on anterior surface 3. Partial wedge on lateral side
UCT/ 18/ 27	Anterior	194	20.62	13.74	20.36	13.22	3.94	3.04	2.96	4.02	7124.59 2967	Yes	1. Transverse fracture 2. Partial wedge	86.18	1. Minimal shatter at impact point 2. Partial wedge on medial side 3. Linear lines on anterior and posterior sides
UCT/ 18/ 28	Anterior	195	20.88	13.62	20.56	13.32	4.02	3..92	3.42	3.36	7641.03 0496	No	N/A	N/A	N/A
UCT/ 18/ 29	Anterior	170	20.46	13.94	18.44	13.26	3.94	3.82	3.46	3.96	6748.23 9692	No	N/A	N/A	N/A
UCT/ 18/ 30	Anterior	184	19.42	13.48	19.22	13.52	3.84	3.12	3.72	4.02	5360.99 016	Yes	1. Shatter 2. Transverse fracture 3. Complete wedge	46.76	1. Shatter at point of impact 2. Complete wedge on medial side
UCT/ 18/ 31	Anterior	178	19.08	13.06	18.24	14.18	4.02	3.18	3.34	2.94	5077.49 3083	Yes	1. Transverse fracture 2. Partial lunate	28.54	1. Shatter at point of impact 2. Linear fracture on anterior side 3. Partial lunate on medial side
UCT/ 18/ 32	Anterior	188	18.74	13.98	18.82	12.92	2.76	2.86	3.34	3.24	4179.09 285	Yes	1. Comminution	101.58	1. Linear fracture on anterior side 2. Clearly defined compression surfaces
UCT/ 18/ 33	Anterior	197	21.02	14.52	20.74	14.26	3.94	2.86	3.58	3.32	7401.07 5967	Yes	1. Transverse fracture 2. Partial lunate	67.96	1. Flaking present 2. Partial lunate on postero-lateral side
UCT/ 18/ 34	Posterior	196	22.06	14.72	19.96	13.54	3.56	3.14	3.54	3.44	9320.34 2801	Yes	1. Transverse fracture 2. Bone chip	12.58	1. Jagged compression surface 2. Square bone chip on lateral side
UCT/ 18/ 35	Posterior	169	18.44	3.28	16.62	9.98	5.04	3.74	3.54	3.64	5669.94 1805	Yes	1. Transverse fracture 2. Partial wedge	22.76	1. Partial wedge on medial side
UCT/ 18/ 36	Posterior	171	19.42	12.16	18.04	12.46	3.42	2.76	2.94	3.74	5908.53 2149	Yes	1. Comminution	N/A	1. Extreme shatter
UCT/ 18/ 37	Posterior	184	20.62	14.02	20.26	13.54	3.22	3.34	4.72	4.38	6977.56 4814	Yes	1. Transverse fracture 2. Bone chip	23.94	1. Square bone chip on medial side

UCT/ 18/ 38	Posterior	186	21.54	13.52	20.28	13.04	3.02	3.18	2.88	3.28	8926.900089	Yes	1. Transverse fracture	N/A	1. Clearly defined compressive surface at point of impact
UCT/ 18/ 39	Posterior	193	23.84	N/A	21.28	N/A	3.34	3.14	3.22	4.12	0	Yes	1. Extreme comminution	N/A	1. Extensive shattering
UCT/ 18/ 40	Posterior	194	22.52	15.58	21.18	14.32	4.72	3.52	3.54	3.78	9733.074638	Yes	1. Transverse fracture 2. Partial wedge	29.32	1. Partial wedge on antero-lateral side 2. Shatter at point of impact
UCT/ 18/ 41	Posterior	193	20.22	14.72	19.28	14.26	3.02	3.68	2.66	3.34	5900.671129	Yes	1. Extreme comminution	77.94	1. Extensive shattering
UCT/ 18/ 42	Posterior	176	17.26	11.08	16.84	10.86	3.34	2.86	3.02	3.38	3616.62842	Yes	1. Extreme comminution 2. Partial wedge	N/A	1. Partial wedge on antero-medial side
UCT/ 18/ 43	Posterior	179	20.02	11.18	18.18	12.06	4.34	3.24	3.22	4.42	7118.547585	Yes	1. Transverse fracture 2. Bone chip	29.02	1. Compression surfaces clearly defined